

# Relating relative Rényi entropies and Wigner-Yanase-Dyson skew information to generalized multiple quantum coherences

Diego Paiva Pires,<sup>1</sup> Augusto Smerzi,<sup>2</sup> and Tommaso Macrì<sup>1,3</sup>

<sup>1</sup>*Departamento de Física Teórica e Experimental,  
Universidade Federal do Rio Grande do Norte, 59072-970 Natal, Rio Grande do Norte, Brazil*

<sup>2</sup>*QSTAR, CNR-INO and LENS, Largo Enrico Fermi 2, I-50125 Firenze, Italy*

<sup>3</sup>*International Institute of Physics, Federal University of Rio Grande do Norte,  
Campus Universitário, Lagoa Nova, Natal-RN 59078-970, Brazil*

Quantum coherence is a crucial resource for quantum information processing. By employing the language of coherence orders largely applied in NMR systems, quantum coherence has been currently addressed in terms of multiple quantum coherences (MQCs). Here we investigate the  $\alpha$ -MQCs, a novel class of multiple quantum coherences which is based on  $\alpha$ -relative purity, an information-theoretic quantifier analogous to quantum fidelity and closely related to Rényi relative entropy of order  $\alpha$ . Our framework enables linking  $\alpha$ -MQCs to Wigner-Yanase-Dyson skew information (WYDSI), an asymmetry monotone finding applications in quantum thermodynamics and quantum metrology. Furthermore, we derive a family of bounds on  $\alpha$ -MQCs, particularly showing that  $\alpha$ -MQC define a lower bound to quantum Fisher information (QFI). We illustrate these ideas for quantum systems described by single-qubit states, two-qubit Bell-diagonal states, and a wide class of multiparticle mixed states. Finally, we investigate the time evolution of the  $\alpha$ -MQC spectrum and the overall signal of relative purity, by simulating the time reversal dynamics of a many-body all-to-all Ising Hamiltonian and comment on applications to physical platforms such as NMR systems, trapped ions, and ultracold atoms.

## I. INTRODUCTION

Quantum coherence is a primary signature of quantum mechanics. It plays, together with entanglement, a central role in quantum technologies [1] as well as in fundamental physics, including quantum thermodynamics [2, 3], quantum phase transitions [4, 5], and quantum biology [6, 7]. Modern approaches include the formulation of quantum coherence within an axiomatic resource theory [8]. Quantum coherence can also be addressed through the framework of multiple quantum coherences (MQCs), also known as coherence orders, which were introduced in the eighties in the context of nuclear magnetic resonance (NMR) [9, 10]. MQCs finds applications ranging from solid-state spectroscopy [11–14] to many-body localization effects induced by decoherence [15], entanglement witnessing [16], and quantum metrology [17].

Noteworthy, it has been recently proved that MQCs provide a useful criterion to probe the buildup of entanglement in quantum many-body systems with long-range interactions [18]. Furthermore, MQCs have also contributed to elucidate the role played by coherence orders into the delocalization of quantum information signaled by out-of-time-order correlation functions (OTOCs), recently measured with a quantum simulator implementing the time-reversal dynamics of a fully connected Ising model [19]. Linking MQC and OTOC have triggered experimental investigations ranging from many-body localization in solid-state spin systems [20–22] to prethermalization effects emerging in the non-equilibrium dynamics in a NMR quantum simulator [23, 24], and also distinguishing effects of scrambling from decoherence [25].

Despite the growing interest into MQCs, little is known about its connection with higher order Rényi entropies,

or even the relation of the second Rényi entropy and MQCs. The situation is also unclear for  $\alpha$ -Rényi relative entropies ( $\alpha$ -RRE), which take an important role in quantum thermodynamics [26–28], quantum communication [29], coherence quantifiers [30–33], and Gaussian states [34]. So far, promising theoretical achievements discussed the feasibility of probing entanglement by measuring Rényi entropies which, up to now, remains a challenge [35–38]. Typically, experimental results mainly focus on second order Rényi entropy by exploiting its relationship with quantum purity of the many-body system [39]. Indeed, significant progress have been made in measuring second order Rényi entropy of a four-site Bose-Hubbard system [40], the two-site Fermi-Hubbard model on trapped ion simulator [41], and the quantum long-range XY model [42]. Further results include measuring Rényi entropy of order  $\alpha = 2, 3, 4$  in the context of quench dynamics of bosons in 1D optical lattices [43].

Here we promote a study of multiple quantum coherences and the buildup of correlations in quantum many-body systems via  $\alpha$ -Rényi relative entropy. We focus on the so-called  $\alpha$ -relative purity, a distinguishability measure of quantum states intimately linked to the Rényi relative entropy of order  $\alpha$  (see details in Sec. II). Motivated by the language of coherence orders developed in NMR and recently addressed under the viewpoint of resource theories, here we will present a novel class of MQCs, called  $\alpha$ -MQCs, which is rooted on  $\alpha$ -RRE. Our framework unveils the link among MQCs,  $\alpha$ -RRE, and Wigner-Yanase-Dyson skew information (WYDSI), an information-theoretic quantifier introduced half century ago and which plays a role on the theory of asymmetry. Noteworthy, it has been shown that WYDSI also witnesses the role of classical and quantum fluctu-

ations in many-body systems [44]. We derive bounds on  $\alpha$ -MQCs, proving that  $\alpha$ -MQCs is upper bounded by quantum Fisher information (QFI), a paradigmatic figure of merit widely applied for enhanced phase estimation [45], and the detection the metrologically useful entanglement [46, 47].

The paper is organized as follows. In Sec. II we review useful basic concepts regarding Rényi relative entropies ( $\alpha$ -RREs) and highlight their main features. In Sec. III we address the concept of coherence orders and derive a novel class of Multiple Quantum Coherences ( $\alpha$ -MQCs) linked to  $\alpha$ -RREs. In Sec. IV we prove that  $\alpha$ -RRE is perturbatively linked to WYDSI. Furthermore, we show that WYDSI testifies the coherence encapsulated in a quantum state by proving its connection with  $\alpha$ -MQCs. In Sec. V we derive a family of upper and lower bounds to the second moment of  $\alpha$ -MQC and WYDSI. In Sec. VI we illustrate our findings. Sections VIA and VIB provide analytical results for single-qubit states and two-qubit Bell-diagonal states, respectively. In Sec. VIC we focus on systems of  $N$ -particle states, and thus present analytical calculations and numerical simulations to support our theoretical predictions. Section VID examines  $\alpha$ -MQC in the context of time-reversing the many-body dynamics of a long-range Ising model. Finally, in Sec. VII we summarize our conclusions.

## II. RÉNYI RELATIVE ENTROPY: A SHORT REVIEW

In this section we will briefly review some basic properties of quantum Rényi relative entropies. Here we will focus on a physical system described by finite-dimensional Hilbert space  $\mathcal{H}$ , i.e.,  $\dim \mathcal{H} = d$ . For completeness, let  $\mathcal{B}(\mathcal{H})$  be the set of linear operators acting over  $\mathcal{H}$ . The state of the system will be given by the density matrix  $\varrho \in \mathcal{S}$ , where  $\mathcal{S} = \{\rho \in \mathcal{H} \mid \rho^\dagger = \rho, \rho \geq 0, \text{Tr}(\rho) = 1\}$  denotes the convex space of positive semi-definite density operators. In this setting, given two states  $\rho, \varrho \in \mathcal{S}$  and  $\alpha \in (0, 1) \cup (1, +\infty)$ , the quantum  $\alpha$ -Rényi relative entropy ( $\alpha$ -RRE) is defined by [48–51]

$$D_\alpha(\rho \parallel \varrho) = \begin{cases} (\alpha - 1)^{-1} \ln [f_\alpha(\rho, \varrho)] & , \text{ if } \text{supp } \rho \subseteq \text{supp } \varrho \\ +\infty & , \text{ otherwise} \end{cases} \quad (1)$$

with the relative purity

$$f_\alpha(\rho, \varrho) := \text{Tr}(\rho^\alpha \varrho^{1-\alpha}) . \quad (2)$$

Here  $\text{supp } X$  stands for the support of  $X \in \mathcal{S}$ . In particular, for  $\alpha \in (0, 1)$  the restriction  $\text{supp } \rho \subseteq \text{supp } \varrho$  is equivalent to  $\rho \not\perp \varrho$ , i.e., whenever  $\text{supp } \rho \cap \text{supp } \varrho$  contains at least one non-zero vector [52]. The positivity of  $\alpha$ -RRE follows from Hölder's inequality for any  $\rho, \varrho \in \mathcal{S}$ , and its monotonicity yields that, for  $\alpha \in (0, 1) \cup (1, 2)$ , one has  $D_\alpha(\mathcal{E}(\varrho) \parallel \mathcal{E}(\omega)) \leq D_\alpha(\varrho \parallel \omega)$ , where  $\mathcal{E}(\bullet)$  denotes a completely positive and trace preserving (CPTP) map [53].

Except for the case  $\alpha = 1/2$ , Rényi relative entropy is not a symmetric information measure and does not define a metric over the space of quantum states. Noteworthy, for  $\alpha \geq 1$  Rényi  $\alpha$ -relative entropy fulfills the Csiszár-Pinsker inequality,  $D_\alpha(\varrho \parallel \rho) \geq (1/2) \|\rho - \varrho\|_1^2$ , where the notation  $\|A\|_1 = \text{Tr}|A|$  stands for the trace norm, with  $|A| := \sqrt{A^\dagger A}$  [54–56]. Moreover, it has been proved that  $\alpha$ -RRE also satisfies a family of Pinsker-type inequalities for  $\alpha \in (0, 1)$  [57]. Finally, we also notice the similarity between the  $\alpha$ -RRE and the so-called sandwiched quantum Rényi relative entropy proposed in Refs. [51, 58].

The functional  $f_\alpha(\rho, \varrho)$  defines the  $\alpha$ -relative purity and it is bounded as  $0 \leq f_\alpha(\rho, \varrho) \leq 1$  [59]. The property  $f_{1-\alpha}(\varrho, \rho) = f_\alpha(\rho, \varrho)$  for all  $\rho, \varrho \in \mathcal{S}$  and  $0 < \alpha < 1$  implies that  $\alpha$ -RRE is skew symmetric for

$$\alpha D_{1-\alpha}(\rho \parallel \varrho) = (1 - \alpha) D_\alpha(\varrho \parallel \rho). \quad (3)$$

In particular, Eq. (2) reduces to  $f_\alpha(\rho, \rho) = 1$  for all  $\alpha$  and  $\rho \in \mathcal{S}$ , and  $\alpha$ -RRE is identically zero in such case. Remarkably, for  $0 \leq \alpha \leq 1$  one may verify that relative purity is also lower bounded by the trace norm (or Schatten 1-norm) as  $f_\alpha(\rho, \varrho) \geq 1 - (1/2) \|\rho - \varrho\|_1$  [60], which collapses into the Powers-Størmer's inequality for  $\alpha = 1/2$  [61, 62].

We summarize some limiting cases of  $\alpha$ -RRE. For  $\alpha = 1$ , Eq. (1) recovers the so-called Umegaki's relative entropy,  $D_1(\rho \parallel \varrho) = \text{Tr}[\rho(\ln \rho - \ln \varrho)]$ , also known as quantum relative entropy or Kullback-Leibler divergence [63, 64]. Furthermore,  $\alpha = 0$  sets the min-relative entropy  $D_{\min}(\rho \parallel \varrho) = -\ln[\text{Tr}(\Xi_\rho \varrho)]$ , with  $\Xi_\rho$  being the projector onto the support of  $\rho$ , while the max-entropy  $D_{\max}(\rho \parallel \varrho) = \inf\{\lambda \in \mathbb{R} \mid \rho \leq \exp(\lambda)\varrho\}$  is obtained for  $\alpha \rightarrow \infty$  if the kernel of  $\varrho$  is contained in the kernel of state  $\rho$  [65].

## III. $\alpha$ -MULTIPLE QUANTUM COHERENCES

In the following we will present the framework to address a novel family of multiple quantum coherences which is related to the relative purity  $f_\alpha(\rho, \varrho)$  defined in Eq. (2). Unless otherwise stated, from now on we will set  $0 < \alpha < 1$ . Let us define the density operator

$$\rho^{(\alpha)} := c_\alpha \rho^\alpha , \quad (4)$$

where  $c_\alpha^{-1} = \text{Tr}(\rho^\alpha)$  is a positive real number. Using the spectral decomposition  $\rho = \sum_l p_l |\psi_l\rangle\langle\psi_l|$ , with  $\langle\psi_l|\psi_r\rangle = \delta_{l,r}$ ,  $0 < p_l < 1$ , and  $\sum_l p_l = 1$ , one may readily conclude that  $c_\alpha^{-1} = \sum_l p_l^\alpha > 0$ .

To formulate the concept of coherence orders, we need first to fix some preferred basis of states [9, 10]. Thus, given the observable  $\hat{A} \in \mathcal{B}(\mathcal{H})$ , let us denote by  $\{|\ell\rangle\}_{\ell=1,\dots,d}$  its complete set of eigenstates, and  $\{\lambda_\ell\}_{\ell=1,\dots,d}$  the corresponding set of discrete eigenvalues. In the remainder of the paper, we will refer to this basis of states as the *reference basis*. We furthermore assume

that the spacing of the eigenvalues of the spectrum of  $\hat{A}$  is an integer  $m \in \mathbb{Z}$

$$\lambda_j - \lambda_\ell = m, \quad (5)$$

for all  $j, \ell \in \{1, \dots, d\}$ . The coherence order decomposition of the density operator  $\rho^{(\alpha)}$  reads

$$\rho^{(\alpha)} = \sum_m \rho_m^{(\alpha)}, \quad (6)$$

where we define

$$\rho_m^{(\alpha)} := \sum_{\lambda_j - \lambda_\ell = m} \langle j | \rho^{(\alpha)} | \ell \rangle | j \rangle \langle \ell |. \quad (7)$$

One should note that Eq. (7) allows us to write down the density matrix  $\rho^{(\alpha)}$  as a sum of non-Hermitian blocks  $\rho_m^{(\alpha)}$  in terms of the reference basis. In other words,  $\rho_m^{(\alpha)}$  contains all coherences between eigenstates  $|j\rangle$  and  $|\ell\rangle$  of  $\hat{A}$  such that  $\lambda_j - \lambda_\ell = m$ , with  $m \in \mathbb{Z}$ .

Noteworthy,  $\rho_m^{(\alpha)}$  satisfies three crucial properties.

- (1) The block  $\rho_m^{(\alpha)}$  is asymmetric with respect to index  $m$  under conjugate transposition, i.e.,

$$(\rho_m^{(\alpha)})^\dagger = \rho_{-m}^{(\alpha)}. \quad (8)$$

- (2) The blocks  $\rho_m^{(\alpha)}$  and  $\rho_n^{(\beta)}$  are orthogonal according to the Hilbert-Schmidt inner product as

$$\langle \rho_m^{(\alpha)}, \rho_n^{(\beta)} \rangle_{\text{HS}} = \delta_{m,n} \langle \rho_m^{(\alpha)}, \rho_m^{(\beta)} \rangle_{\text{HS}}. \quad (9)$$

where we define  $\langle A, B \rangle_{\text{HS}} := \text{Tr}(A^\dagger B)$ , for  $A, B \in \mathcal{B}(\mathcal{H})$ .

- (3) By considering the observable  $\hat{A}$  which generates the translationally-covariant operation  $\mathcal{U}_\phi(\bullet) := e^{-i\phi\hat{A}} \bullet e^{i\phi\hat{A}}$ , with  $\phi \in (0, 2\pi]$ , thus block  $\rho_m^{(\alpha)}$  acquires a phase shift that reads

$$\mathcal{U}_\phi(\rho_m^{(\alpha)}) = e^{-im\phi} \rho_m^{(\alpha)}. \quad (10)$$

Note that  $\rho_0^{(\alpha)}$  is incoherent under such a phase encoding process, i.e., the subspace related to the mode of coherence  $m = 0$  is translationally symmetric with respect to  $\hat{A}$  [66]. For details in the proof of Eqs. (8)–(10), see Appendix A.

In the following we will discuss how the relative purity  $f_\alpha(\rho, \rho_\phi)$  of states  $\rho$  and  $\rho_\phi = \mathcal{U}_\phi(\rho)$  behaves under the framework of coherence orders. From Eq. (10), one may verify that

$$\rho_\phi^\alpha = c_\alpha^{-1} \sum_m \mathcal{U}_\phi(\rho_m^{(\alpha)}) = c_\alpha^{-1} \sum_m e^{-im\phi} \rho_m^{(\alpha)}, \quad (11)$$

where we used the property  $\rho_\phi^\alpha = [\mathcal{U}_\phi(\rho)]^\alpha = \mathcal{U}_\phi(\rho^\alpha)$ , which holds for  $0 < \alpha < 1$  [67, 68]. Crucially, Eq. (11) implies that the unitary evolution imprints a phase shift

on each block  $\rho_m^{(\alpha)}$  built from the coherence orders decomposition of the probe state  $\rho$ . Hence, from Eqs. (6), (9), and (11), the relative purity becomes

$$\begin{aligned} f_\alpha(\rho, \rho_\phi) &= (c_\alpha c_{1-\alpha})^{-1} \sum_{m,n} e^{-im\phi} \text{Tr} \left( \rho_n^{(\alpha)} \rho_m^{(1-\alpha)} \right) \\ &= (c_\alpha c_{1-\alpha})^{-1} \sum_m e^{-im\phi} I_m^\alpha(\rho), \end{aligned} \quad (12)$$

where  $I_m^\alpha(\rho)$  is the  $\alpha$ -Multiple-Quantum Intensity ( $\alpha$ -MQI) defined as

$$I_m^\alpha(\rho) = \text{Tr} \left( (\rho_m^{(\alpha)})^\dagger \rho_m^{(1-\alpha)} \right). \quad (13)$$

The set  $\{I_m^\alpha(\rho)\}_{m \in \mathbb{Z}}$  is called  $\alpha$ -MQI spectrum. Quite remarkably, the asymmetry property presented in Eq. (8) implies that  $\alpha$ -MQI satisfies the following algebraic identities

$$[I_m^\alpha(\rho)]^* = I_m^{1-\alpha}(\rho) = I_{-m}^\alpha(\rho). \quad (14)$$

Furthermore, setting  $\phi = 0$  into Eq. (12), it is straightforward to verify that the sum of all  $\alpha$ -MQI relative to state  $\rho$ , fulfills the normalization constraint

$$\sum_m I_m^\alpha(\rho) = c_\alpha c_{1-\alpha}. \quad (15)$$

We emphasize that one may access the  $\alpha$ -MQI  $I_m^\alpha(\rho)$  by Fourier transforming Eq. (12) with respect to  $\phi \in (0, 2\pi]$ , which reads

$$I_m^\alpha(\rho) = \frac{c_\alpha c_{1-\alpha}}{2\pi} \int_0^{2\pi} d\phi e^{im\phi} f_\alpha(\rho, \rho_\phi). \quad (16)$$

It should be noted that  $\alpha$ -MQI defined in Eq. (13) is analogous to the standard MQI addressed by Gärttner *et al.* [18, 19]. However, it turns out the framework developed here covers the subtle case of coherence orders involving rational powers  $\rho^\alpha$  of the density operator, with  $0 < \alpha < 1$ .

It is worth mentioning that relative purity  $f_\alpha(\rho, \rho_\phi)$  implies a nontrivial constraint involving  $\alpha$ -MQI and  $\alpha$ -Rényi relative entropy. Indeed, by substituting Eq. (12) into Eq. (1), one obtains

$$\begin{aligned} D_\alpha(\rho \| \rho_\phi) &= \frac{\alpha}{\alpha-1} S_{1-\alpha}(\rho) - S_\alpha(\rho) \\ &\quad + \frac{1}{\alpha-1} \ln \left( \sum_m e^{-im\phi} I_m^\alpha(\rho) \right), \end{aligned} \quad (17)$$

where  $S_\alpha(\rho)$  is the standard Rényi entropy

$$S_\alpha(\rho) := \frac{1}{1-\alpha} \ln [\text{Tr}(\rho^\alpha)]. \quad (18)$$

In summary, Eq. (17) means that, to distinguish states  $\rho$  and  $\rho_\phi$  through  $\alpha$ -Rényi relative entropy, one requires the knowledge of Rényi entropy  $S_\alpha(\rho)$  and the  $\alpha$ -MQI spectrum of state  $\rho$  with respect to the reference basis of generator  $\hat{A}$ .

#### IV. BRIDGING RÉNYI RELATIVE ENTROPY, $\alpha$ -MQC, AND WIGNER-YANASE-DYSON SKEW INFORMATION

In this Section we study the connection between the  $\alpha$ -RRE, the WDSI, and the  $\alpha$ -MQC.

##### A. $\alpha$ -RRE and WYDSI

Let us consider the protocol of Fig. 1, where the parameter  $\phi$  is imprinted on the probe state  $\rho \in \mathcal{S}$  through the unitary evolution  $\mathcal{U}_\phi(\bullet) := e^{-i\phi\hat{A}} \bullet e^{i\phi\hat{A}}$ , where  $\hat{A} \in \mathcal{B}(\mathcal{H})$  is a generic observable. In general, the problem of estimating the phase shift  $\phi$  is addressed via the so-called Cramér-Rao bound [69, 70], which relates the inverse of quantum Fisher information (QFI) to the maximum phase sensitivity achievable for state  $\rho$  undergoing the referred physical process. Furthermore, estimating such unknown parameter is also a task related to the ability of distinguishing both states  $\rho$  and  $\rho_\phi = \mathcal{U}_\phi(\rho)$  [71]. In this context, one typically introduces the Bures distance or another suitable *bona fide* quantifier also related to the Uhlmann-Jozsa fidelity [72]. Here we will adopt the  $\alpha$ -RRE introduced in Sec. II as a figure of merit to distinguish quantum states. By performing a Taylor expansion of  $\alpha$ -RRE up to second order in  $\phi$  around  $\phi = 0$ , one obtains

$$D_\alpha(\rho\|\rho_\phi) \approx -\frac{\phi^2}{\alpha-1} \mathcal{I}_\alpha(\rho, \hat{A}) + O(\phi^3), \quad (19)$$

where we define

$$\mathcal{I}_\alpha(\rho, \hat{A}) := -\frac{1}{2} \text{Tr} \left( [\hat{A}, \rho^\alpha] [\hat{A}, \rho^{1-\alpha}] \right). \quad (20)$$

Interestingly, Eq. (20) defines the so-called Wigner-Yanase-Dyson skew information (WYDSI) [73]. WYDSI is positive,  $\mathcal{I}_\alpha(\rho, \hat{A}) \geq 0$ , and a convex quantity [74, 75], i.e.,  $\mathcal{I}_\alpha(\gamma\rho + (1-\gamma)\varrho, \hat{A}) \leq \gamma\mathcal{I}_\alpha(\rho, \hat{A}) + (1-\gamma)\mathcal{I}_\alpha(\varrho, \hat{A})$ , for all  $0 < \alpha < 1$  and  $0 \leq \gamma \leq 1$ , with  $\rho, \varrho \in \mathcal{S}$  and  $\hat{A} \in \mathcal{B}(\mathcal{H})$ . Furthermore, WYDSI is additive for product states, i.e.,  $\mathcal{I}_\alpha(\rho_1 \otimes \rho_2, \hat{A}_1 \otimes \mathbb{I} + \mathbb{I} \otimes \hat{A}_2) = \mathcal{I}_\alpha(\rho_1, \hat{A}_1) + \mathcal{I}_\alpha(\rho_2, \hat{A}_2)$  [76]. Physically, WYDSI quantifies the non-commutativity of operator  $\hat{A}$  regarding to the quantum state  $\rho$ . Noteworthy, WYDSI has been also recognized as an asymmetry measure [66, 77]. Moreover, WYDSI also appears in a slightly modified quantum version of the work dissipation fluctuation relation in nonequilibrium quantum thermodynamics [78, 79]. In particular, for  $\alpha = 1/2$ , WYDSI reduces to the so-called Wigner-Yanase skew information (WYSI), which is defined as  $\mathcal{I}_{1/2}(\rho, \hat{A}) = -(1/2) \text{Tr}([\sqrt{\rho}, \hat{A}]^2)$ . In Appendix B we show that, for  $\alpha \rightarrow 1$ , Eq. (19) is well behaved and reduces to  $D_1(\rho\|\rho_\phi) = \lim_{\alpha \rightarrow 1} D_\alpha(\rho\|\rho_\phi) \approx \phi^2 \left( \text{Tr}(\hat{A}^2 \rho \ln \rho) - \text{Tr}(\hat{A} \rho \hat{A} \ln \rho) \right) + O(\phi^3)$ .

The proof of Eq. (19) goes as follows. Given the states  $\rho$  and  $\rho_\phi = e^{-i\phi\hat{A}} \rho e^{i\phi\hat{A}}$ , with  $\text{supp } \rho \subseteq \text{supp } \rho_\phi$ , we know

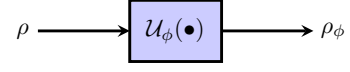


FIG. 1. (Color online) Schematic depiction of the quantum protocol.

from Sec. II that  $D_\alpha(\rho\|\rho_\phi) = (\alpha-1)^{-1} \ln [f_\alpha(\rho, \rho_\phi)]$ , with  $f_\alpha(\rho, \rho_\phi) = \text{Tr}(\rho^\alpha \rho_\phi^{1-\alpha})$ . The Taylor expansion of  $\alpha$ -RRE up to second order in  $\phi$ , around  $\phi = 0$ , is given by

$$D_\alpha(\rho\|\rho_\phi) \approx [D_\alpha(\rho\|\rho_\phi)]_{\phi=0} + \phi [D'_\alpha(\rho\|\rho_\phi)]_{\phi=0} + \frac{\phi^2}{2} [D''_\alpha(\rho\|\rho_\phi)]_{\phi=0} + O(\phi^3), \quad (21)$$

where the notation  $\mathcal{A}'$ ,  $\mathcal{A}''$  stand for the derivatives  $d\mathcal{A}/d\phi$ , and  $d^2\mathcal{A}/d\phi^2$ , respectively. We notice that  $[D_\alpha(\rho\|\rho_\phi)]_{\phi=0} = 0$  since  $\rho_0 = \rho$ . Moreover, both the first and the second order derivatives of  $\alpha$ -RRE with respect to  $\phi$  can be written as

$$[D'_\alpha(\rho\|\rho_\phi)]_{\phi=0} = \frac{1}{\alpha-1} (f'_\alpha(\rho, \rho_\phi))_{\phi=0}, \quad (22)$$

and

$$[D''_\alpha(\rho\|\rho_\phi)]_{\phi=0} = \frac{1}{\alpha-1} \left[ f''_\alpha(\rho, \rho_\phi) - (f'_\alpha(\rho, \rho_\phi))^2 \right]_{\phi=0}, \quad (23)$$

where we have used that  $\lim_{\phi \rightarrow 0} f_\alpha(\rho, \rho_\phi) = 1$ . In order to compute Eqs. (22) and (23), we need to evaluate the derivatives  $f'_\alpha(\rho, \rho_\phi)$  and  $f''_\alpha(\rho, \rho_\phi)$  at  $\phi = 0$ . To do so, one may prove that the quantum state  $\rho_\phi = e^{-i\phi\hat{A}} \rho e^{i\phi\hat{A}}$  evolving unitarily implies that  $\rho_\phi^s = [\mathcal{U}_\phi(\rho)]^s = \mathcal{U}_\phi(\rho^s)$ , for  $0 < s < 1$  (see Appendix A in Ref. [68]). Therefore, it follows that the  $k$ th order derivative of state  $\rho_\phi^s$  becomes

$$\frac{d^k}{d\phi^k} \rho_\phi^s = (-i)^k \underbrace{[\hat{A}, [\hat{A}, \dots, [\hat{A}, \rho_\phi^s] \dots]]}_{k \text{ times}}. \quad (24)$$

Hence, starting from Eq. (24), both first and second order derivatives of the relative purity at the vicinity of  $\phi = 0$  are given by

$$\begin{aligned} (f'_\alpha(\rho, \rho_\phi))_{\phi=0} &= i \left[ \text{Tr} \left( \hat{A} [\rho^\alpha, \rho_\phi^{1-\alpha}] \right) \right]_{\phi=0} \\ &= 0, \end{aligned} \quad (25)$$

and

$$\begin{aligned} (f''_\alpha(\rho, \rho_\phi))_{\phi=0} &= \left[ \text{Tr} \left( [\hat{A}, \rho^\alpha] [\hat{A}, \rho_\phi^{1-\alpha}] \right) \right]_{\phi=0} \\ &= -2 \mathcal{I}_\alpha(\rho, \hat{A}), \end{aligned} \quad (26)$$

respectively, where  $\mathcal{I}_\alpha(\rho, \hat{A})$  is the WYDSI defined in Eq. (20). Substituting Eqs. (25) and (26) into Eqs. (22) and (23), it yields  $[D'_\alpha(\rho\|\rho_\phi)]_{\phi=0} = 0$  and also

$$[D''_\alpha(\rho\|\rho_\phi)]_{\phi=0} = -\frac{2}{\alpha-1} \mathcal{I}_\alpha(\rho, \hat{A}). \quad (27)$$



Finally, by plugging these results into Eq. (21), one recovers the Taylor expansion of  $\alpha$ -RRE aforementioned in Eq. (19). It should be noted that a similar conclusion was previously reported in the context of resource theory of asymmetry, but focusing on the Taylor expansion of relative purity [80].

## B. WYDSI and $\alpha$ -MQC

Remarkably, WYDSI captures information about the coherence order decomposition of state  $\rho$  with respect to the reference basis of the observable  $\hat{A}$ . Indeed, one may prove that

$$4 c_\alpha c_{1-\alpha} \mathcal{I}_\alpha(\rho, \hat{A}) = F_I^\alpha(\rho, \hat{A}), \quad (28)$$

where here  $F_I^\alpha(\rho, \hat{A})$  denotes the second moment of the  $\alpha$ -MQC spectrum defined by

$$F_I^\alpha(\rho, \hat{A}) := 2 \sum_m m^2 I_m^\alpha(\rho). \quad (29)$$

In order to prove such statement, we will take advantage from the framework of coherence orders discussed in Sec. III. Starting from the definition of WYDSI in Eq. (20), one may write down

$$\mathcal{I}_\alpha(\rho, \hat{A}) = -\frac{1}{2 c_\alpha c_{1-\alpha}} \sum_{m,n} \text{Tr} \left( [\hat{A}, \rho_n^{(\alpha)}] [\hat{A}, \rho_m^{(1-\alpha)}] \right), \quad (30)$$

where we have used that  $\rho = c_s^{-1} \sum_m \rho_m^{(s)}$  (see Eqs. (4) and (6)). Now, note that each commutator in Eq. (30) can be conveniently simplified according to the identity below

$$\begin{aligned} [\hat{A}, \rho_m^{(s)}] &= \sum_{\lambda_j - \lambda_\ell = m} \langle j | \rho^{(s)} | \ell \rangle [\hat{A}, |j\rangle\langle\ell|] \\ &= \sum_{\lambda_j - \lambda_\ell = m} \underbrace{(\lambda_j - \lambda_\ell)}_m \langle j | \rho^{(s)} | \ell \rangle |j\rangle\langle\ell| \\ &= m \rho_m^{(s)}, \end{aligned} \quad (31)$$

which descends from  $\hat{A}|j\rangle = \lambda_j|j\rangle$ . Moreover, from Eqs. (9) and (13) we also know that

$$\begin{aligned} \text{Tr} \left( \rho_n^{(\alpha)} \rho_m^{(1-\alpha)} \right) &= \delta_{n,-m} \text{Tr} \left( \rho_{-m}^{(\alpha)} \rho_m^{(1-\alpha)} \right) \\ &= \delta_{n,-m} I_m^\alpha(\rho). \end{aligned} \quad (32)$$

Finally, by substituting Eqs. (31) and (32) into Eq. (30), one arrives to the result indicated in Eq. (28).

We point out that one could obtain the same result as in Eq. (28) by simply taking the second order derivative of  $\alpha$ -RRE in Eq. (17) at  $\phi = 0$ . Quite interestingly, it is possible to verify that  $F_I^\alpha(\rho, \hat{A})$  is a real number. Indeed, we know from Eq. (14) that  $[I_m^\alpha(\rho)]^* = I_{-m}^\alpha(\rho)$ ,

Therefore, by taking the complex conjugate of Eq. (29), one obtains

$$\begin{aligned} [F_I^\alpha(\rho, \hat{A})]^* &= 2 \sum_m m^2 [I_m^\alpha(\rho)]^* \\ &= 2 \sum_m m^2 I_{-m}^\alpha(\rho) \\ &= F_I^\alpha(\rho, \hat{A}). \end{aligned} \quad (33)$$

where we applied the substitution  $m \rightarrow -m$  over the summation label.

Equation (28) is one of the main results of the paper. To be more specific, in Refs. [18, 19, 81] the second moment of MQC spectrum is obtained from quantum fidelity, also called relative purity, i.e., the overlap between states  $\rho_0$  and  $\rho_\phi$ , which in turn define a lower bound on quantum Fisher information (QFI). Notwithstanding, addressing quantum relative Rényi entropy as a *bona fide* distinguishability measure of mixed states, here we derive the novel class of  $\alpha$ -Multiple-Quantum Intensity,  $I_m^\alpha(\rho)$  (see Eq. (13)). In turn,  $\alpha$ -MQI implies the second moment of  $\alpha$ -MQC spectrum,  $F_I^\alpha(\rho, \hat{A})$  (see Eq. (29)), which play the role of  $\alpha$ -curvature. We also proved that  $F_I^\alpha(\rho, \hat{A})$  is related to WYDSI (see Eq. (28)), a widely established asymmetry measure in the context of resource theories [66, 77], which also captures the signature of quantum fluctuations in many-body systems at finite temperature [44]. This means that, by bridging Rényi relative entropy,  $\alpha$ -MQC, and Wigner-Yanase-Dyson skew information, one provides an alternative perspective to the understanding of quantum fluctuations and quantum correlations.

## V. BOUNDS ON $\alpha$ -MQC

In this section we will establish a novel class of bounds on WYDSI that naturally holds for the second moment of  $\alpha$ -Multiple Quantum Intensity. We introduce the lower bound

$$F_I^\alpha(\rho, \hat{A}) \geq 8 \alpha(1-\alpha) c_\alpha c_{1-\alpha} \mathcal{I}^L(\rho, \hat{A}), \quad (34)$$

where

$$\mathcal{I}^L(\rho, \hat{A}) := -\frac{1}{4} \text{Tr}([\rho, \hat{A}]^2). \quad (35)$$

that we prove in Appendix C. For the case  $\alpha = 1/2$ , Eq. (34) becomes

$$F_I^{1/2}(\rho, \hat{A}) \geq 2 c_{1/2}^2 \mathcal{I}^L(\rho, \hat{A}). \quad (36)$$

Importantly, quantifier  $\mathcal{I}^L(\rho, \hat{A})$  have been introduced in the context of quantum coherence characterization, thus defining a lower bound on Wigner-Yanase skew information, i.e.,  $\mathcal{I}_{1/2}(\rho, \hat{A}) \geq \mathcal{I}^L(\rho, \hat{A})$  [82]. Recently, a detection scheme to measure  $\mathcal{I}^L$  was implemented in an all-optical experiment [83, 84]. Eq. (36) generalizes

this bound by providing a less tight lower bound to the quantity  $F_I^{1/2}(\rho, \hat{A})$ . To see this, note that Eq. (28) becomes  $F_I^{1/2}(\rho, \hat{A}) = 4c_{1/2}^2 \mathcal{I}_{1/2}(\rho, \hat{A})$  for  $\alpha = 1/2$ , which allow us to recast Eq. (36) into the form  $\mathcal{I}_{1/2}(\rho, \hat{A}) \geq (1/2)\mathcal{I}^L(\rho, \hat{A})$ . Hence, the latter inequality differs from the bound  $\mathcal{I}_{1/2}(\rho, \hat{A}) \geq \mathcal{I}^L(\rho, \hat{A})$  by a factor 1/2 and does not set the tightest lower bound.

An upper bound on WYDSI and thus on the second moment of  $\alpha$ -Multiple Quantum Intensity can be derived using the inequalities  $\mathcal{I}_\alpha(\rho, \hat{A}) \leq \mathcal{I}_{1/2}(\rho, \hat{A}) \leq \mathcal{V}_{1/2}(\rho, \hat{A})$ , and  $\mathcal{I}_\alpha(\rho, \hat{A}) \leq \mathcal{V}_\alpha(\rho, \hat{A}) \leq \mathcal{V}_{1/2}(\rho, \hat{A})$ , respectively [85]. Therefore  $F_I^\alpha(\rho, \hat{A})$  fulfills the two inequalities

$$\frac{F_I^\alpha(\rho, \hat{A})}{4c_\alpha c_{1-\alpha}} \leq \mathcal{I}_{1/2}(\rho, \hat{A}) \leq \mathcal{V}_{1/2}(\rho, \hat{A}), \quad (37)$$

and

$$\frac{F_I^\alpha(\rho, \hat{A})}{4c_\alpha c_{1-\alpha}} \leq \mathcal{V}_\alpha(\rho, \hat{A}) \leq \mathcal{V}_{1/2}(\rho, \hat{A}), \quad (38)$$

where  $\mathcal{V}_\alpha(\rho, \hat{A})$  denotes the  $\alpha$ -variance

$$\mathcal{V}_\alpha(\rho, \hat{A}) := \sqrt{[V(\rho, \hat{A})]^2 - [V(\rho, \hat{A}) - \mathcal{I}_\alpha(\rho, \hat{A})]^2}, \quad (39)$$

and  $V(\rho, \hat{A})$  stands for the variance

$$V(\rho, \hat{A}) = \text{Tr}(\rho \hat{A}^2) - [\text{Tr}(\rho \hat{A})]^2. \quad (40)$$

It is worth emphasizing that inequalities in Eqs. (38) and (39) cannot be recasted in a single inequality. In fact, upon varying  $\alpha$ , there exists intervals over the range  $0 < \alpha < 1$  in which  $\mathcal{I}_{1/2}(\rho, \hat{A}) \geq \mathcal{V}_\alpha(\rho, \hat{A})$ , and others in which  $\mathcal{I}_{1/2}(\rho, \hat{A}) \leq \mathcal{V}_\alpha(\rho, \hat{A})$ . For more details, see Sec. VIC, particularly panels in Figs. 3, 4 and 5.

We are now in position to derive a novel class of hierarchical bounds on the second moment of  $\alpha$ -Multiple Quantum Intensity. In fact, one may bring together inequalities given in Eqs. (34), (37) and (38) and thus combine them to produce a general family of bounds on  $F_I^\alpha(\rho, \hat{A})$ . Therefore, one straightforwardly gets

$$2\alpha(1-\alpha)\mathcal{I}^L(\rho, \hat{A}) \leq \frac{F_I^\alpha(\rho, \hat{A})}{4c_\alpha c_{1-\alpha}} \leq \mathcal{I}_{1/2}(\rho, \hat{A}) \leq \mathcal{V}_{1/2}(\rho, \hat{A}), \quad (41)$$

and also

$$2\alpha(1-\alpha)\mathcal{I}^L(\rho, \hat{A}) \leq \frac{F_I^\alpha(\rho, \hat{A})}{4c_\alpha c_{1-\alpha}} \leq \mathcal{V}_\alpha(\rho, \hat{A}) \leq \mathcal{V}_{1/2}(\rho, \hat{A}). \quad (42)$$

### A. Bounds on the Quantum Fisher Information

From now on we shall prove that  $F_I^\alpha(\rho, \hat{A})$  defines a lower bound on quantum Fisher information (QFI).

We begin by recalling the standard setup for phase-estimation based on QFI. Given a finite-dimensional quantum system undergoing a unitary evolution to the output state  $\rho_\phi = e^{-i\phi\hat{A}}\rho e^{i\phi\hat{A}}$ , generated by the observable  $\hat{A}$ , then QFI related to estimating the phase shift  $\phi$  encoded into the probe state  $\rho = \sum_j p_j |\psi_j\rangle\langle\psi_j|$  reads [84, 86]

$$\mathcal{F}_Q(\rho, \hat{A}) = \frac{1}{2} \sum_{j,l=1}^d \frac{(p_j - p_l)^2}{p_j + p_l} |\langle\psi_j|\hat{A}|\psi_l\rangle|^2, \quad (43)$$

where  $d = \dim\mathcal{H}$  is the Hilbert space dimension,  $0 < p_j < 1$ , and the sum runs over all the indices  $\{j, l\}$  such that  $p_j + p_l \neq 0$ . In comparison to standard definitions of QFI (see Refs. [18, 84, 86]), note that Eq. (43) includes an extra normalizing factor 1/4 and guarantees that QFI recovers the variance of generator  $\hat{A}$  for pure states [87–89]. To proceed deriving the novel upper bound to  $F_I^\alpha(\rho, \hat{A})$ , we point out that  $\mathcal{I}_{1/2}(\rho, \hat{A})$  is also related to QFI according to the inequality  $\mathcal{I}_{1/2}(\rho, \hat{A}) \leq \mathcal{F}_Q(\rho, \hat{A}) \leq 2\mathcal{I}_{1/2}(\rho, \hat{A})$  [88, 89]. Therefore, by substituting the latter into Eq. (41), it is possible to show a strict bound involving the second moment of  $\alpha$ -MQI and QFI, which reads

$$\frac{F_I^\alpha(\rho, \hat{A})}{4c_\alpha c_{1-\alpha}} \leq \mathcal{I}_{1/2}(\rho, \hat{A}) \leq \mathcal{F}_Q(\rho, \hat{A}) \leq 2\mathcal{I}_{1/2}(\rho, \hat{A}). \quad (44)$$

Equation (44) is one of the main results of the paper. It provides a family of lower bounds on QFI,  $\mathcal{F}_Q(\rho, \hat{A})$ , which in turn depend on Wigner-Yanase skew information,  $\mathcal{I}_{1/2}(\rho, \hat{A})$ , and also on the second moment of  $\alpha$ -MQC spectrum,  $F_I^\alpha(\rho, \hat{A})$ . Importantly, this result paves the way for a discussion of entanglement characterization by using  $\alpha$ -multiple quantum coherences from  $\alpha$ -Rényi relative entropies. More in general, Eq. (44) defines a novel criterion for detecting entanglement in a mixed many-body state.

## VI. EXAMPLES

In this Section we present some examples to illustrate our main findings. In Sec. VIA, by considering the paradigmatic case of a single qubit state, we obtain analytical expressions for  $\alpha$ -MQI spectrum  $I_m^\alpha(\rho)$  and also  $F_I^\alpha(\rho, \hat{A})$ . In Sec. VIB we discuss  $\alpha$ -MQCs for the case of two-qubit Bell-diagonal states. Moving to the multipartite scenario, Sec. VIC presents numerical analysis for  $\alpha$ -MQI spectrum related to a class of mixed entangled states, viz., uniform superposition state, Greenberger-Horne-Zeilinger state (GHZ-state), and Werner state (W-state). Finally, Sec. VID discusses  $\alpha$ -MQI spectrum for a physical scenario in which the referred class of multipartite states evolves under a time-reversal quantum protocol.

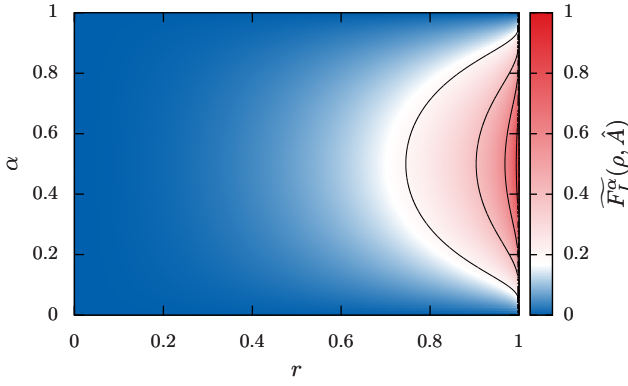


FIG. 2. (Color online) Density plot of figure of merit  $\widehat{F}_I^\alpha(\rho, \hat{A})$  for  $\hat{n} = \{0, 0, 1\}$  and  $\hat{r} = \{\cos \varphi, \sin \varphi, 0\}$ , with  $\tilde{\mathbf{G}} := (\mathbf{G} - \min\{\mathbf{G}\}) / (\max\{\mathbf{G}\} - \min\{\mathbf{G}\})$ , and  $F_I^\alpha(\rho, \hat{A})$  is given in Eq. (52). In this case, since vectors  $\hat{n}$  and  $\vec{r}$  are orthogonal,  $F_I^\alpha(\rho, \hat{A})$  does not depend on the azimuthal angle  $\varphi$ , and thus it is solely function of  $r$  and  $\alpha$ .

### A. Single qubit state

Let us consider the quantum system described by  $\rho = (1/2)(\mathbb{I} + \vec{r} \cdot \vec{\sigma})$ , i.e., the Bloch sphere representation of the single qubit mixed state, where  $\vec{\sigma} = (\sigma_x, \sigma_y, \sigma_z)$  is the vector of Pauli matrices,  $\vec{r} = r \hat{r}$  is the Bloch vector, with  $\hat{r} = \{\sin \theta \cos \varphi, \sin \theta \sin \varphi, \cos \theta\}$ ,  $0 < r < 1$ ,  $\theta \in [0, \pi]$  and  $\varphi \in [0, 2\pi[$ , while  $\mathbb{I}$  is the  $2 \times 2$  identity matrix. Here we will choose the operator  $\hat{A} = (1/2)(\hat{n} \cdot \vec{\sigma})$  as the generator of the phase encoding protocol, where  $\hat{n} = \{n_x, n_y, n_z\}$  is a unit vector with  $n_x^2 + n_y^2 + n_z^2 = 1$ . In this case, the reference basis is composed by the eigenstates  $\{|+\rangle, |-\rangle\}$  of  $\hat{A}$  defined as

$$|\pm\rangle = \frac{1}{\sqrt{2}} \left( \pm \sqrt{1 \pm n_z} |0\rangle + \frac{n_x + i n_y}{\sqrt{1 \pm n_z}} |1\rangle \right), \quad (45)$$

where  $|0\rangle = [1 \ 0]^T$  and  $|1\rangle = [0 \ 1]^T$  are the vectors defining the computational basis states in the complex two-dimensional vector space  $\mathbb{C}^2$ , where we have that  $\hat{A}|\pm\rangle = \lambda_\pm|\pm\rangle$ , with eigenvalues  $\lambda_\pm = \pm 1/2$ .

One may verify that, for  $0 < \alpha < 1$ , operator  $\rho^{(\alpha)}$  in Eq. (4) is given by

$$\rho^{(\alpha)} = \frac{1}{2} [\mathbb{I} + (1 - 2^{1-\alpha}(1-r)^\alpha c_\alpha) (\hat{r} \cdot \vec{\sigma})], \quad (46)$$

and

$$c_\alpha^{-1} = 2^{-\alpha} [(1+r)^\alpha + (1-r)^\alpha]. \quad (47)$$

Starting from Eq. (46), the coherence orders decomposition reads  $\rho^{(\alpha)} = \sum_m \rho_m^{(\alpha)}$  with  $m = \{-1, 0, +1\}$ . The non-Hermitian matrix blocks  $\rho_m^{(\alpha)}$  are given by

$$\rho_{\pm 1}^{(\alpha)} = \frac{1}{4} (1 - 2^{1-\alpha}(1-r)^\alpha c_\alpha) [(\hat{n} \times \vec{\sigma}) \cdot (\hat{n} \times \hat{r}) \pm i(\hat{n} \times \hat{r}) \cdot \vec{\sigma}], \quad (48)$$

TABLE I. Analytical expressions for the family of theoretical-information quantifiers related the single qubit mixed state.

Quantifier	Analytical value
$\mathcal{I}^L(\rho, \hat{A})$	$(r^2/8) [1 - (\hat{n} \cdot \hat{r})^2]$
$\mathcal{F}_Q(\rho, \hat{A})$	$(r^2/4) [1 - (\hat{n} \cdot \hat{r})^2]$
$V(\rho, \hat{A})$	$(1/4) [1 - (\hat{n} \cdot \vec{r})^2]$
$\mathcal{I}_{1/2}(\rho, \hat{A})$	$(1/4) (1 - \sqrt{1 - r^2}) [1 - (\hat{n} \cdot \hat{r})^2]$

and

$$\rho_0^{(\alpha)} = \frac{1}{2} [\mathbb{I} + (1 - 2^{1-\alpha}(1-r)^\alpha c_\alpha) (\hat{n} \cdot \hat{r}) (\hat{n} \cdot \vec{\sigma})]. \quad (49)$$

Based on Eqs. (48) and (49), one readily conclude that  $\text{Tr}(\rho_m^{(\alpha)}) = \delta_{m,0}$  and  $\rho_{-1}^{(\alpha)} = (\rho_{+1}^{(\alpha)})^\dagger$ . Therefore,  $\alpha$ -Multiple Quantum Intensity defined in Eq. (13) becomes

$$I_{\pm 1}^\alpha(\rho) = \frac{1}{4} (2 c_\alpha c_{1-\alpha} - 1) [1 - (\hat{n} \cdot \hat{r})^2], \quad (50)$$

and

$$I_0^\alpha(\rho) = \frac{1}{2} [1 + (2 c_\alpha c_{1-\alpha} - 1) (\hat{n} \cdot \hat{r})^2]. \quad (51)$$

Furthermore, note that if vectors  $\hat{n}$  and  $\hat{r}$  are parallel, then we have  $I_{\pm 1}^\alpha(\rho) = 0$  and  $I_0^\alpha(\rho) = c_\alpha c_{1-\alpha}$ . Conversely, if vectors  $\hat{n}$  and  $\hat{r}$  are orthogonal, it follows that  $I_{\pm 1}^\alpha(\rho) = (1/4)(2 c_\alpha c_{1-\alpha} - 1)$  and  $I_0^\alpha(\rho) = 1/2$ . Finally, from Eqs. (50) and (51) the second moment of  $\alpha$ -MQI (see Eq. (29)) is written as

$$F_I^\alpha(\rho, \hat{A}) = (2 c_\alpha c_{1-\alpha} - 1) [1 - (\hat{n} \cdot \hat{r})^2]. \quad (52)$$

Let us now analyze the behaviour of the second moment of  $\alpha$ -MQI in Eq. (52). Naturally,  $F_I^\alpha(\rho, \hat{A})$  inherits some properties from  $\alpha$ -MQI. On the one hand, when vectors  $\hat{n}$  and  $\hat{r}$  are orthogonal, i.e.,  $\hat{n} \cdot \hat{r} = 0$ , thus  $F_I^\alpha(\rho, \hat{A})$  depends uniquely on Bloch sphere radius  $r$  and the parameter  $\alpha$ . For instance, this case is illustrated in Fig. 2 choosing vector  $\hat{n} = \{0, 0, 1\}$  related to the generator  $\hat{A} = (1/2)\sigma_z$ , and  $\hat{r} = \{\cos \varphi, \sin \varphi, 0\}$  denoting the single qubit mixed state lying in the equatorial  $xy$ -plane of the Bloch sphere. On the other hand, when vectors  $\hat{n}$  and  $\hat{r}$  parallel, we have that  $F_I^\alpha(\rho, \hat{A})$  vanishes. For completeness, in Table I we summarize analytical expressions, obtained by using the single qubit state  $\rho = (1/2)(\mathbb{I} + \vec{r} \cdot \vec{\sigma})$  and generator  $\hat{A} = (1/2)(\hat{n} \cdot \vec{\sigma})$ , for the functional  $\mathcal{I}^L(\rho, \hat{A})$ , quantum Fisher information  $\mathcal{F}_Q(\rho, \hat{A})$ , standard variance  $V(\rho, \hat{A})$ , and also Wigner-Yanase skew information  $\mathcal{I}_{1/2}(\rho, \hat{A})$ .

## B. Bell-diagonal states

Let us now consider the class of two-qubit states with maximally mixed marginals represented by the Bell-diagonal states [90]

$$\rho_{\text{BD}} = \frac{1}{4} \left( \mathbb{I} \otimes \mathbb{I} + \sum_{j=x,y,z} a_j \sigma_j \otimes \sigma_j \right), \quad (53)$$

where  $\mathbb{I}$  is the  $2 \times 2$  identity matrix,  $\sigma_j$  is the  $j$ th Pauli matrix, and the coefficients  $a_j = \text{Tr}[\rho(\sigma_j \otimes \sigma_j)] \in [-1, 1]$  denote the triple  $\vec{a} = \{a_x, a_y, a_z\}$ , which uniquely identifies the Bell-diagonal state. In particular, for  $|a_x| + |a_y| + |a_z| \leq 1$  we thus have  $\rho$  as a separable state [91]. Here we will choose the generator  $\hat{A} = \hat{n} \cdot \vec{S}$ , where  $\hat{n} = \{n_x, n_y, n_z\}$  is a unit vector with  $n_x^2 + n_y^2 + n_z^2 = 1$ , and  $\vec{S} = \{\hat{S}_x, \hat{S}_y, \hat{S}_z\}$  is the angular momentum vector, with  $\hat{S}_j = (1/2)(\sigma_j \otimes \mathbb{I} + \mathbb{I} \otimes \sigma_j)$  for  $j \in \{x, y, z\}$ . The reference basis  $\{|\ell\rangle\}_{\ell=1,\dots,4}$  contains the eigenstates of  $\hat{A}$  given by

$$\begin{aligned} |1\rangle &= \frac{1}{\sqrt{2}}(|0, 1\rangle - |1, 0\rangle) \\ |2\rangle &= -\frac{1}{\sqrt{2}} \left[ \frac{n_- (n_- |0, 0\rangle - \sqrt{2} n_z |L\rangle)}{\sqrt{1 - n_z^2}} - \sqrt{1 - n_z^2} |1, 1\rangle \right] \\ |3\rangle &= \frac{1}{2} \left( \frac{n_-^2}{1 + n_z} |0, 0\rangle - \sqrt{2} n_- |L\rangle + (1 + n_z) |1, 1\rangle \right) \\ |4\rangle &= \frac{1}{2} \left( \frac{n_-^2}{1 - n_z} |0, 0\rangle + \sqrt{2} n_- |L\rangle + (1 - n_z) |1, 1\rangle \right) \end{aligned} \quad (54)$$

with  $n_{\pm} := n_x \pm i n_y$ , and  $|L\rangle := (1/\sqrt{2})(|0, 1\rangle + |1, 0\rangle)$ . Note that  $\hat{A}|\ell\rangle = \lambda_{\ell}|\ell\rangle$ , where  $\lambda_1 = \lambda_2 = 0$ ,  $\lambda_3 = -1$ ,  $\lambda_4 = 1$ , and thus one obtains  $m \in \{\pm 2, \pm 1, 0\}$ .

Given the Bell-diagonal state, one may verify that, for  $0 < \alpha < 1$ , the operator  $\rho_{\text{BD}}^{(\alpha)} = c_{\alpha}(\rho_{\text{BD}})^{\alpha}$  (cf. Eq. (4)) becomes

$$\rho_{\text{BD}}^{(\alpha)} = \frac{1}{4} \left( \mathbb{I} \otimes \mathbb{I} + \sum_{j=x,y,z} \eta_{\alpha,j} \sigma_j \otimes \sigma_j \right), \quad (55)$$

with

$$\begin{aligned} \eta_{\alpha,j} &:= c_{\alpha} [-v_1^{\alpha} + (1 - 2\delta_{j,z})v_2^{\alpha} \\ &\quad + (1 - 2\delta_{j,y})v_3^{\alpha} + (1 - 2\delta_{j,x})v_4^{\alpha}] , \end{aligned} \quad (56)$$

for  $j \in \{x, y, z\}$ , and also

$$c_{\alpha}^{-1} = v_1^{\alpha} + v_2^{\alpha} + v_3^{\alpha} + v_4^{\alpha} . \quad (57)$$

Here  $\{v_r\}_{r=1,\dots,4}$  denote the set of eigenvalues of the two-qubit Bell-diagonal state, where

$$\begin{aligned} v_r &= \frac{1}{4} [1 - (1 - 2\delta_{r,2} - 2\delta_{r,3})a_x \\ &\quad + (1 - 2\delta_{r,1} - 2\delta_{r,3})a_y + (1 - 2\delta_{r,1} - 2\delta_{r,2})a_z] . \end{aligned} \quad (58)$$

TABLE II. Analytical expressions for the family of theoretical-information quantifiers related to the Bell-diagonal state and generator  $\hat{A} = \hat{n} \cdot \vec{S}$ , where  $\hat{n} = \{n_x, n_y, n_z\}$  is a unit vector with  $n_x^2 + n_y^2 + n_z^2 = 1$ , and  $\vec{S} = \{\hat{S}_x, \hat{S}_y, \hat{S}_z\}$  is the angular momentum vector, with  $\hat{S}_j = (1/2)(\sigma_j \otimes \mathbb{I} + \mathbb{I} \otimes \sigma_j)$  for  $j \in \{x, y, z\}$ . Note that sum runs over index  $j, k, l \in \{x, y, z\}$ , and  $|\vec{a}|^2 = a_x^2 + a_y^2 + a_z^2$ .

Quantifier	Analytical value
$\mathcal{I}^L(\rho_{\text{BD}}, \hat{A})$	$\frac{1}{16} \left( 2 \vec{a} ^2 - \sum_{j \neq k \neq l} (a_j^2 + 2a_k a_l) n_j^2 \right)$
$\mathcal{F}_Q(\rho_{\text{BD}}, \hat{A})$	$\frac{1}{4} \sum_{j \neq k \neq l} \frac{((a_k - a_l) n_j)^2}{(1 + a_j)}$
$V(\rho_{\text{BD}}, \hat{A})$	$\frac{1}{2} \left( 1 + \sum_j a_j n_j^2 \right)$
$\mathcal{I}_{1/2}(\rho_{\text{BD}}, \hat{A})$	$\frac{1}{8} \sum_{j \neq k \neq l} n_j^2 (\eta_{1/2,k} - \eta_{1/2,l})^2$

Based on Eq. (55), one may evaluate the non-Hermitian blocks  $(\rho_{\text{BD}}^{(\alpha)})_m$  appearing into the coherence orders decomposition  $\rho_{\text{BD}}^{(\alpha)} = \sum_m (\rho_{\text{BD}}^{(\alpha)})_m$ , and thus determine the  $\alpha$ -Multiple Quantum Intensity spectrum  $\{I_m^{\alpha}(\rho_{\text{BD}})\}$ , with  $m \in \{0, \pm 1, \pm 2\}$ . We will not show them here as the expressions are cumbersome. After a lengthy calculation the expression for  $\alpha$ -MQI yields

$$F_I^{\alpha}(\rho_{\text{BD}}, \hat{A}) = \sum_{j \neq k \neq l} n_j^2 (\eta_{\alpha,k} - \eta_{\alpha,l})(\eta_{1-\alpha,k} - \eta_{1-\alpha,l}) , \quad (59)$$

where the sum run over index  $j, k, l \in \{x, y, z\}$ . Noteworthy, Eq. (59) collapses into the particular cases (i)  $F_I^{\alpha}(\rho_{\text{BD}}, \hat{S}_x) = (\eta_{\alpha,y} - \eta_{\alpha,z})(\eta_{1-\alpha,y} - \eta_{1-\alpha,z})$  for  $\hat{n} = \{1, 0, 0\}$ ; (ii)  $F_I^{\alpha}(\rho_{\text{BD}}, \hat{S}_y) = (\eta_{\alpha,x} - \eta_{\alpha,z})(\eta_{1-\alpha,x} - \eta_{1-\alpha,z})$  for  $\hat{n} = \{0, 1, 0\}$ ; and (iii)  $F_I^{\alpha}(\rho_{\text{BD}}, \hat{S}_z) = (\eta_{\alpha,x} - \eta_{\alpha,y})(\eta_{1-\alpha,x} - \eta_{1-\alpha,y})$  for  $\hat{n} = \{0, 0, 1\}$ .

In Table II we list the analytical expressions obtained for the functional  $\mathcal{I}^L(\rho_{\text{BD}}, \hat{A})$ , quantum Fisher information  $\mathcal{F}_Q(\rho_{\text{BD}}, \hat{A})$ , standard variance  $V(\rho_{\text{BD}}, \hat{A})$ , and also Wigner-Yanase skew information  $\mathcal{I}_{1/2}(\rho_{\text{BD}}, \hat{A})$ .

## C. Multiparticle states

In this Section we study multiparticle systems of  $N$ -qubit states belonging to the  $d$ -dimensional Hilbert space  $\mathcal{H}_d$ , with  $d = 2^N$ . We consider three prototypical examples of states which are well known in quantum information. From now on we will choose the collective spin operator  $\hat{A} = \hat{n} \cdot \vec{S}$ , where  $\hat{n} = \{n_x, n_y, n_z\}$  is a unit vector with  $n_x^2 + n_y^2 + n_z^2 = 1$ , and  $\vec{S} = \{\hat{S}_x, \hat{S}_y, \hat{S}_z\}$  is the angular momentum vector, with

$$\hat{S}_{x,y,z} = \frac{1}{2} \sum_{l=1}^N \mathbb{I}^{\otimes l-1} \otimes \sigma_l^{x,y,z} \otimes \mathbb{I}^{\otimes N-l} . \quad (60)$$



TABLE III. Family of theoretical-information quantifiers  $\mathcal{I}^L$ , quantum Fisher information  $\mathcal{F}_Q$ , variance  $V$ , and Wigner-Yanase skew information  $\mathcal{I}_{1/2}$ . Here we have evaluated these quantities by considering the following operator pairs (i)  $(\rho_{\text{eqn}}, \hat{S}_z)$ , (ii)  $(\rho_{\text{GHZ}}, \hat{S}_z)$ , and (iii)  $(\rho_{\text{W}}, \hat{S}_x)$ , where  $\rho_{\text{eqn}}$ ,  $\rho_{\text{GHZ}}$  and  $\rho_{\text{W}}$  denote the  $N$ -particle states in Eqs. (61), (69), and (75), respectively, with  $d = 2^N$ . The collective spin operators  $\hat{S}_x$ ,  $\hat{S}_z$  are defined in Eq. (60).

Quantifier	$(\rho_{\text{eqn}}, \hat{S}_z)$	$(\rho_{\text{GHZ}}, \hat{S}_z)$	$(\rho_{\text{W}}, \hat{S}_x)$
$\mathcal{I}^L$	$\frac{1}{8} N p^2$	$\frac{1}{8} N^2 p^2$	$\frac{1}{8} (4 + 3(N - 2)) p^2$
$\mathcal{F}_Q$	$N \frac{d p^2}{4(2+(d-2)p)}$	$N^2 \frac{d p^2}{4(2+(d-2)p)}$	$(3N - 2) \frac{d p^2}{4(2+(d-2)p)}$
$V$	$\frac{1}{4} N$	$\frac{1}{4} N^2$	$\frac{1}{4} (N + 2(N - 1)p)$
$\mathcal{I}_{1/2}$	$\frac{N}{4d} \left( \sqrt{1 + (d-1)p} - \sqrt{1-p} \right)^2$	$\frac{N^2}{4d} \left( \sqrt{1 + (d-1)p} - \sqrt{1-p} \right)^2$	$\frac{(3N-2)}{4d} \left( \sqrt{1 + (d-1)p} - \sqrt{1-p} \right)^2$

Let us first set  $\hat{n} = \{0, 0, 1\}$ , i.e.,  $\hat{A} = \hat{S}_z$ , and consider the probe state

$$\rho_{\text{eqn}} = \left( \frac{1-p}{d} \right) \mathbb{I} + p (|+\rangle\langle+|)^{\otimes N}, \quad (61)$$

with  $d = 2^N$ ,  $0 < p < 1$ , and  $|+\rangle = (1/\sqrt{2})(|0\rangle + |1\rangle)$  is the equal superposition state. For  $0 < \alpha < 1$ , we obtain

$$\rho_{\text{eqn}}^{(\alpha)} = c_\alpha \left( \frac{1-p}{d} \right)^\alpha \mathbb{I} + \xi_\alpha(p, d) (|+\rangle\langle+|)^{\otimes N}, \quad (62)$$

where we define

$$c_\alpha^{-1} = (d-1) \left( \frac{1-p}{d} \right)^\alpha + \left( \frac{1+(d-1)p}{d} \right)^\alpha \quad (63)$$

and

$$\xi_\alpha(d, p) := 1 - c_\alpha d^{1-\alpha} (1-p)^\alpha. \quad (64)$$

The coherence orders decomposition  $\rho_{\text{eqn}}^{(\alpha)} = \sum_m (\rho_{\text{eqn}}^{(\alpha)})_m$  into non-Hermitian blocks originates cumbersome expressions that we do not report here. It turns out that the corresponding expressions for the  $\alpha$ -MQI take simple forms. For  $m = 0$  one obtains

$$I_0^\alpha(\rho_{\text{eqn}}) = \frac{1}{d} \left[ 1 + \left( \frac{(2N)!}{d(N!)^2} - 1 \right) \xi_\alpha(d, p) \xi_{1-\alpha}(d, p) \right], \quad (65)$$

while, for  $m \neq 0$ , we have

$$I_m^\alpha(\rho_{\text{eqn}}) = \frac{g_{N,m}}{d^2} \xi_\alpha(d, p) \xi_{1-\alpha}(d, p), \quad (66)$$

where

$$g_{N,m} = \frac{(2N)!}{(N-m)!(N+m)!} \quad (67)$$

is the degeneracy of each block. Therefore, from Eqs. (65) and (66) one may write down

$$F_I^\alpha(\rho_{\text{eqn}}, S_z) = N \xi_\alpha(d, p) \xi_{1-\alpha}(d, p). \quad (68)$$

In Table III we list the expressions of  $\mathcal{I}^L(\rho_{\text{eqn}}, \hat{S}_z)$ , the quantum Fisher information  $\mathcal{F}_Q(\rho_{\text{eqn}}, \hat{S}_z)$ , the standard variance  $V(\rho_{\text{eqn}}, S_z)$ , and the Wigner-Yanase skew information  $\mathcal{I}_{1/2}(\rho_{\text{eqn}}, \hat{S}_z)$ . In Fig. 3 we plot Eq. (68) for the system sizes  $N = 3$ ,  $N = 4$  and  $N = 5$ , and mixing parameter values  $p = 0.25$  and  $p = 0.5$ .

Let us move to a different case. Now, we choose the unit vector  $\hat{n} = \{0, 0, 1\}$ , i.e.,  $\hat{A} = \hat{S}_z$ , and consider the state

$$\rho_{\text{GHZ}} = \left( \frac{1-p}{d} \right) \mathbb{I} + p |\text{GHZ}_N\rangle\langle\text{GHZ}_N|, \quad (69)$$

with  $d = 2^N$ ,  $0 < p < 1$ , and  $|\text{GHZ}_N\rangle$  is the GHZ-state of  $N$  particles defined as

$$|\text{GHZ}_N\rangle = \frac{1}{\sqrt{2}} (|0\rangle^{\otimes N} + |1\rangle^{\otimes N}). \quad (70)$$

Based on Eq. (70), for  $0 < \alpha < 1$ , one may verify that

$$\rho_{\text{GHZ}}^{(\alpha)} = c_\alpha \left( \frac{1-p}{d} \right)^\alpha \mathbb{I} + \xi_\alpha(p, d) |\text{GHZ}_N\rangle\langle\text{GHZ}_N|, \quad (71)$$

where both functions  $c_\alpha$  and  $\xi_\alpha(p, d)$  are the ones defined in Eqs. (63) and (64), respectively. By analogy with the previous example, the expressions for  $\alpha$ -MQI take simple forms. We emphasize that  $\alpha$ -MQI is identically zero for all indices  $m \neq 0$  and  $m \neq \pm N$ . For  $m = 0$  one obtains

$$I_0^\alpha(\rho_{\text{GHZ}}) = c_\alpha c_{1-\alpha} - \frac{1}{2} \xi_\alpha(d, p) \xi_{1-\alpha}(d, p), \quad (72)$$

while, for  $m = \pm N$ , one gets

$$I_{\pm N}^\alpha(\rho_{\text{GHZ}}) = \frac{1}{4} \xi_\alpha(d, p) \xi_{1-\alpha}(d, p), \quad (73)$$

Therefore, from Eqs. (72) and (73) the second moment of  $\alpha$ -MQI is given by

$$F_I^\alpha(\rho_{\text{GHZ}}, S_z) = N^2 \xi_\alpha(d, p) \xi_{1-\alpha}(d, p). \quad (74)$$

In Table III we list the expressions obtained for  $\mathcal{I}^L(\rho_{\text{GHZ}}, S_z)$ , QFI  $\mathcal{F}_Q(\rho_{\text{GHZ}}, S_z)$ , the standard variance  $V(\rho_{\text{GHZ}}, S_z)$ , and the Wigner-Yanase skew information  $\mathcal{I}_{1/2}(\rho_{\text{GHZ}}, S_z)$ . It is worthwhile to note that, fixing the generator  $\hat{A} = \hat{S}_z$  as the collective magnetization along  $z$ -axis,  $F_I^\alpha$  grows quadratically with system size  $N$  for the mixed GHZ-state in Eq. (69), while it grows linearly for the state  $\rho_{\text{eqn}}$  in Eq. (61). In Fig. 4 we plot Eq. (74) for the values of system size  $N = 3$ ,  $N = 4$  and  $N = 5$ , and mixing parameter  $p = 0.25$  and  $p = 0.5$ .

Finally, we turn to our third example. We begin by specifying the unit vector  $\hat{n} = \{1, 0, 0\}$  related to the generator  $\hat{A} = \hat{S}_x$ , and define the probe state

$$\rho_W = \left(\frac{1-p}{d}\right) \mathbb{I} + p |W\rangle\langle W|, \quad (75)$$

where  $d = 2^N$ ,  $0 < p < 1$ , and  $|W\rangle$  is the  $W$ -state of  $N$  particles given by [92]

$$|W\rangle = \frac{1}{\sqrt{N}} \sum_{l=1}^N |0\rangle^{\otimes l-1} \otimes |1\rangle^l \otimes |0\rangle^{\otimes N-l}. \quad (76)$$

For  $0 < \alpha < 1$ , it follows that

$$\rho_W^{(\alpha)} = c_\alpha \left(\frac{1-p}{d}\right)^\alpha \mathbb{I} + \xi_\alpha(p, d) |W\rangle\langle W|, \quad (77)$$

where both functions  $c_\alpha$  and  $\xi_\alpha(p, d)$  are exactly the same as defined in Eqs. (63) and (64), respectively. In spite of the complexity of the expressions of the coherence orders decomposition  $\rho_W^{(\alpha)} = \sum_m (\rho_W^{(\alpha)})_m$ , it is possible to derive analytically the second moment of  $\alpha$ -MQI, which reads

$$F_I^\alpha(\rho_W, S_x) = \left(\frac{3N-2}{d-1}\right) (d c_\alpha c_{1-\alpha} - 1). \quad (78)$$

Table III reports the expressions obtained for  $\mathcal{I}^L(\rho_W, \hat{S}_x)$ , quantum Fisher information  $\mathcal{F}_Q(\rho_W, \hat{S}_x)$ , standard variance  $V(\rho_W, \hat{S}_x)$ , and also Wigner-Yanase skew information  $\mathcal{I}_{1/2}(\rho_W, \hat{S}_x)$ . In Fig. 5 we plot  $F_I^\alpha(\rho_W, \hat{S}_x)$  for the values of system size  $N = 3$ ,  $N = 4$  and  $N = 5$ , and mixing parameter  $p = 0.25$  and  $p = 0.5$ .

#### D. Long-range Quantum Ising model

Now we move to the dynamical scenario and consider the protocol depicted in Fig. 6. Such interferometric scheme is equivalent to the Loschmidt-echo protocol proposed for the creation and detection of entangled non-Gaussian states [93] with an Ising model with long-range interactions recently realized in a dilute gas of Rydberg-dressed cesium atoms [94]. This protocol is also analogous to time-reversal dynamics simulating Loschmidt echo in NMR many-spin systems [95, 96]. The protocol was implemented in a trapped ion quantum simulator, and used to detect the buildup of quantum correlations in many-body systems via multiple quantum coherences [19]. The Hamiltonian of the system is a fully

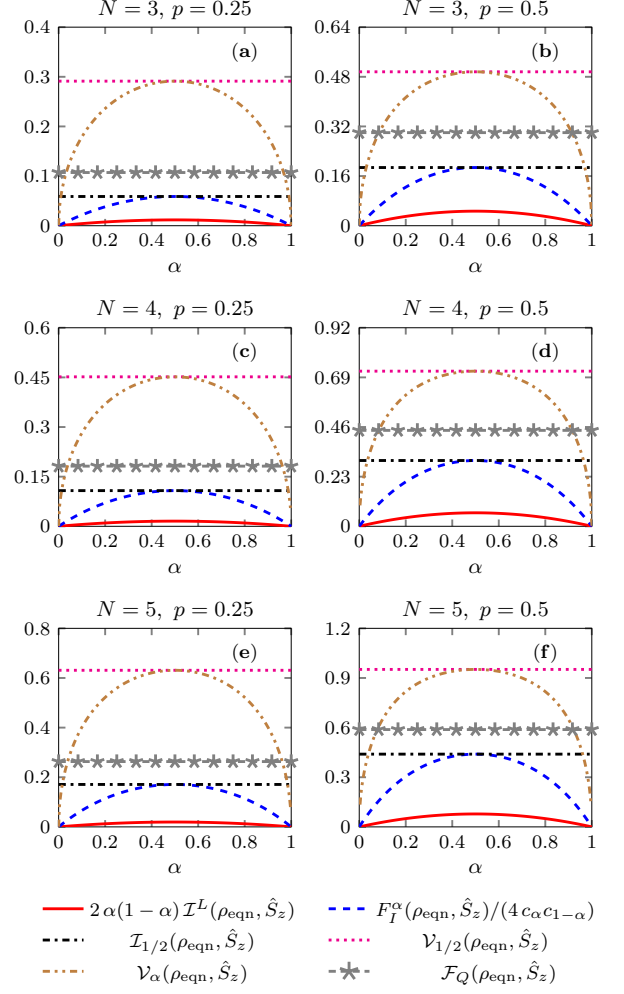


FIG. 3. (Color online) Plot of quantity  $2\alpha(1-\alpha)\mathcal{I}^L(\rho_{\text{eqn}}, \hat{S}_z)$  (red solid line),  $\alpha$ -MQI  $F_I^\alpha(\rho_{\text{eqn}}, \hat{S}_z)/(4c_\alpha c_{1-\alpha})$  (blue dashed line), Wigner-Yanase skew information  $\mathcal{I}_{1/2}(\rho_{\text{eqn}}, \hat{S}_z)$  (black dot dashed line),  $1/2$ -variance  $\mathcal{V}_{1/2}(\rho_{\text{eqn}}, \hat{S}_z)$  (magenta dotted line),  $\alpha$ -variance  $\mathcal{V}_\alpha(\rho_{\text{eqn}}, \hat{S}_z)$  (brown dashed and double-dotted line), and quantum Fisher information  $\mathcal{F}_Q(\rho_{\text{eqn}}, \hat{S}_z)$  (gray star dashed line). Here we choose the mixed state  $\rho_{\text{eqn}} = ((1-p)/2^N) \mathbb{I} + p(|+\rangle\langle +|)^{\otimes N}$ , with  $|+\rangle = (1/\sqrt{2})(|0\rangle + |1\rangle)$ , and the generator  $\hat{S}_z = (1/2) \sum_{l=1}^N \mathbb{I}^{\otimes l-1} \otimes \sigma_l^z \otimes \mathbb{I}^{\otimes N-l}$ , for values (a)  $N = 3$  and  $p = 0.25$ ; (b)  $N = 3$  and  $p = 0.5$ ; (c)  $N = 4$  and  $p = 0.25$ ; (d)  $N = 4$  and  $p = 0.5$ ; (e)  $N = 5$  and  $p = 0.25$ ; and (f)  $N = 5$  and  $p = 0.5$ . In each panel, the plots successfully fulfill the constraints imposed by the chain of bounds given in Eqs. (41), (42), and (44).

connected Ising model

$$H_{zz} = \frac{J}{N} \sum_{j<l} \sigma_j^z \sigma_l^z, \quad (79)$$

where  $J$  is the coupling strength,  $N$  is the number of spins, and  $\sigma_j^z$  are the Pauli spin matrices. For simplicity,

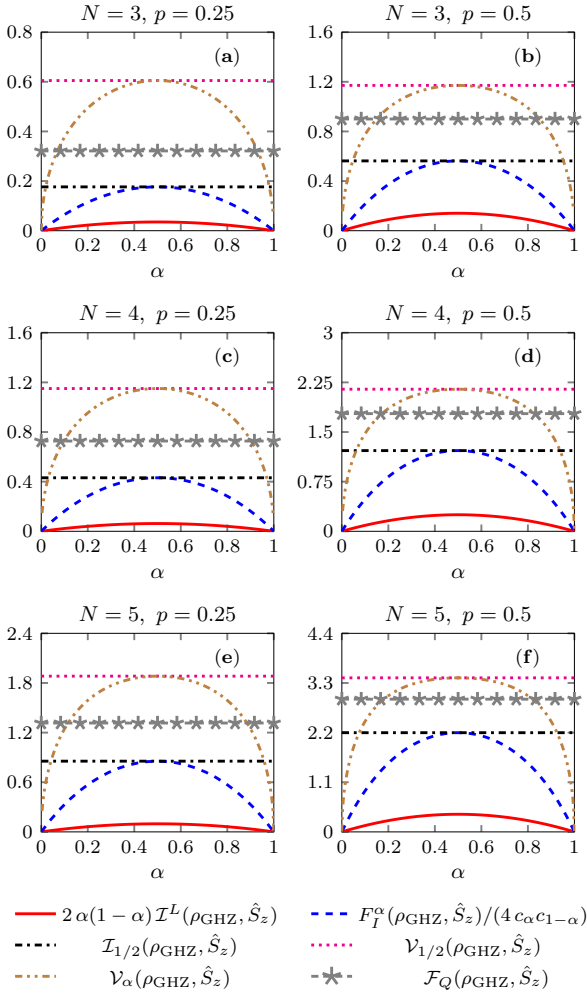


FIG. 4. (Color online) Plot of  $2\alpha(1-\alpha)\mathcal{I}^L(\rho_{\text{GHZ}}, \hat{S}_z)$  (red solid line),  $\alpha$ -MQI  $F_I^\alpha(\rho_{\text{GHZ}}, \hat{S}_z)/(4c_\alpha c_{1-\alpha})$  (blue dashed line), Wigner-Yanase skew information  $\mathcal{I}_{1/2}(\rho_{\text{GHZ}}, \hat{S}_z)$  (black dot dashed line),  $1/2$ -variance  $\mathcal{V}_{1/2}(\rho_{\text{GHZ}}, \hat{S}_z)$  (magenta dotted line),  $\alpha$ -variance  $\mathcal{V}_\alpha(\rho_{\text{GHZ}}, \hat{S}_z)$  (brown dashed and double-dotted line), and quantum Fisher information  $\mathcal{F}_Q(\rho_{\text{GHZ}}, \hat{S}_z)$  (gray star dashed line). Here we choose the mixed state  $\rho_{\text{GHZ}} = ((1-p)/2^N)\mathbb{I} + p|\text{GHZ}_N\rangle\langle\text{GHZ}_N|$ , with  $|\text{GHZ}_N\rangle = (1/\sqrt{2})(|0\rangle^{\otimes N} + |1\rangle^{\otimes N})$ , and the generator  $\hat{S}_z = (1/2)\sum_{l=1}^N \mathbb{I}^{\otimes l-1} \otimes \sigma_l^z \otimes \mathbb{I}^{\otimes N-l}$ , for values (a)  $N = 3$  and  $p = 0.25$ ; (b)  $N = 3$  and  $p = 0.5$ ; (c)  $N = 4$  and  $p = 0.25$ ; (d)  $N = 4$  and  $p = 0.5$ ; (e)  $N = 5$  and  $p = 0.25$ ; and (f)  $N = 5$  and  $p = 0.5$ . In each panel, the plots successfully fulfill the constraints imposed by the chain of bounds given in Eqs. (41), (42), and (44).

the system is initialized in the state

$$\rho_0 = \left(\frac{1-p}{d}\right)\mathbb{I} + p(|+\rangle\langle+|)^{\otimes N}, \quad (80)$$

with  $d = 2^N$ ,  $0 < p < 1$ , and  $|+\rangle = (1/\sqrt{2})(|0\rangle + |1\rangle)$  being the equal superposition state.

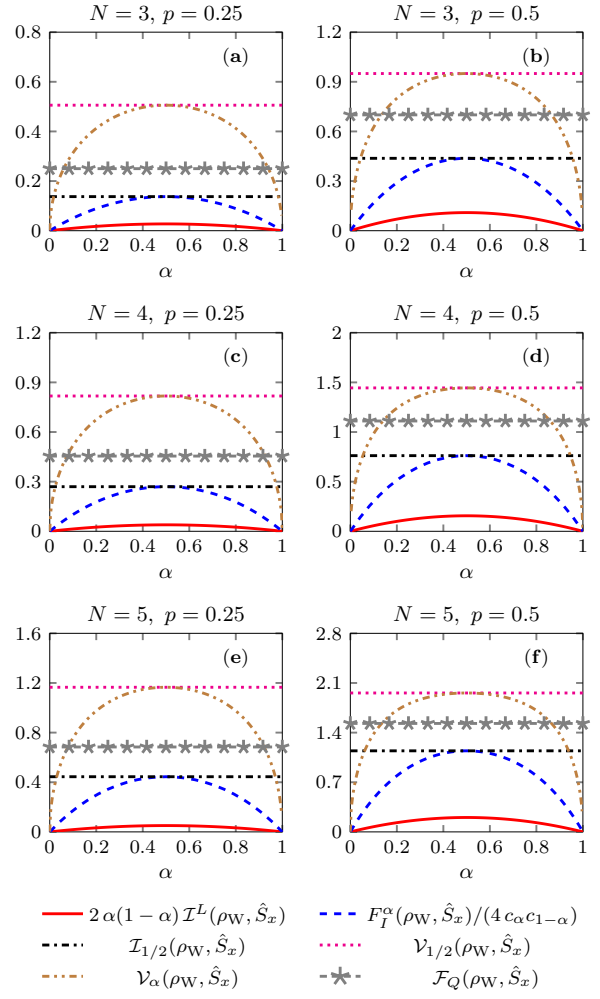


FIG. 5. (Color online) Plot of  $2\alpha(1-\alpha)\mathcal{I}^L(\rho_W, \hat{S}_x)$  (red solid line),  $\alpha$ -MQI  $F_I^\alpha(\rho_W, \hat{S}_x)/(4c_\alpha c_{1-\alpha})$  (blue dashed line), Wigner-Yanase skew information  $\mathcal{I}_{1/2}(\rho_W, \hat{S}_x)$  (black dot dashed line),  $1/2$ -variance  $\mathcal{V}_{1/2}(\rho_W, \hat{S}_x)$  (magenta dotted line),  $\alpha$ -variance  $\mathcal{V}_\alpha(\rho_W, \hat{S}_x)$  (brown dashed and double-dotted line), and quantum Fisher information  $\mathcal{F}_Q(\rho_W, \hat{S}_x)$  (gray star dashed line). Here we choose the mixed state  $\rho_W = ((1-p)/2^N)\mathbb{I} + p|W\rangle\langle W|$ , with  $|W\rangle = (1/\sqrt{N})\sum_{l=1}^N |0\rangle^{\otimes l-1} \otimes |1\rangle^l \otimes |0\rangle^{\otimes N-l}$ , and the generator  $\hat{S}_x = (1/2)\sum_{l=1}^N \mathbb{I}^{\otimes l-1} \otimes \sigma_l^x \otimes \mathbb{I}^{\otimes N-l}$ , for values (a)  $N = 3$  and  $p = 0.25$ ; (b)  $N = 3$  and  $p = 0.5$ ; (c)  $N = 4$  and  $p = 0.25$ ; (d)  $N = 4$  and  $p = 0.5$ ; (e)  $N = 5$  and  $p = 0.25$ ; and (f)  $N = 5$  and  $p = 0.5$ . In each panel, the plots successfully fulfill the constraints imposed by the chain of bounds given in Eqs. (41), (42), and (44).

In the forward step of the protocol of Fig. 6, the initial state  $\rho_0$  of the system evolves unitarily according to  $\mathcal{U}_t = e^{-itH_{zz}}$  and reaches the intermediate state  $\rho_t = \mathcal{U}_t \rho_0 \mathcal{U}_t^\dagger$ . Just to clarify, here we set  $\hbar = 1$ . Subsequently, the operator  $\hat{R}_\phi = e^{-i\phi\hat{S}_x}$  rotates the system about  $x$ -axis, with  $\hat{S}_x = (1/2)\sum_{l=1}^N \mathbb{I}^{\otimes l-1} \otimes \sigma_l^x \otimes \mathbb{I}^{\otimes N-l}$ , and thus the

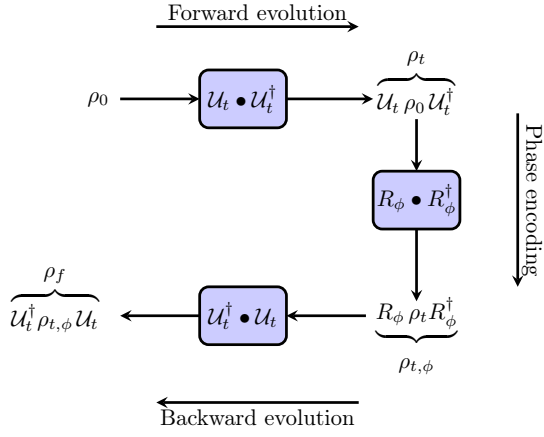


FIG. 6. (Color online) Depiction of the quantum protocol discussed in Section VID. In the forward process, the initial state  $\rho_0$  of the system undergoes a unitary evolution and reaches the intermediate state  $\rho_t = \mathcal{U}_t \rho_0 \mathcal{U}_t^\dagger$ . Then, the operator  $R_\phi$  imprints a phase shift  $\phi$  into  $\rho_t$ , and the system is subsequently described by the state  $\rho_{t,\phi} = R_\phi \rho_t R_\phi^\dagger$ . In the last step of the protocol, the system evolves backward in time according to the reversed unitary dynamics and is finally described by the final state  $\rho_f = \mathcal{U}_t^\dagger \rho_{t,\phi} \mathcal{U}_t$ .

system is characterized by the state  $\rho_{t,\phi} = R_\phi \rho_t R_\phi^\dagger$ . Finally, the system evolves unitarily backward and reaches the final state  $\rho_f = \mathcal{U}_t^\dagger \rho_{t,\phi} \mathcal{U}_t$ . We stress that, in practice, the backward protocol is implemented inverting the sign of  $H$  by changing  $J \rightarrow -J$ .

In the following we will apply  $\alpha$ -relative purity to distinguish input and output states after running the quantum protocol. Interestingly, the relative purity involving states  $\rho_0$  and  $\rho_f$  becomes

$$f_\alpha(\rho_0, \rho_f) = \text{Tr}(\rho_0^\alpha \rho_f^{1-\alpha}) = \text{Tr}(\rho_t^\alpha \rho_{t,\phi}^{1-\alpha}) = f_\alpha(\rho_t, \rho_{t,\phi}), \quad (81)$$

where we have used that  $\rho_f^{1-\alpha} = \mathcal{U}_t^\dagger \rho_{t,\phi}^{1-\alpha} \mathcal{U}_t$ , since  $\mathcal{U}_t$  is a unitary operator [68]. Note that, for  $\phi = 0$ , we thus have  $\rho_{t,0} = \rho_t$  and  $\alpha$ -relative purity is equal to 1. We point out that  $\alpha$ -relative purity will play the role of revival probability exhibited by the quantum system undergoing the time-reversal evolution. Indeed, RHS of Eq. (81) means that, for a nonzero phase shift  $\phi$  encoded into the time-dependent state  $\rho_t$  by the rotation  $R_\phi = e^{-i\phi \hat{S}_x}$  inserted between forward and backward time evolutions, thus the  $\alpha$ -relative purity  $f_\alpha(\rho_t, \rho_{t,\phi})$  will deviate from the unity as a function of time  $t$ . Moreover, such a revival can be interpreted as a signature of the buildup of correlations of the many-body state  $\rho_t$  [19].

According to Eq. (12), one may write the  $\alpha$ -relative purity in terms of the  $\alpha$ -MQI as

$$f_\alpha(\rho_0, \rho_f) = (c_\alpha c_{1-\alpha})^{-1} \sum_m e^{-im\phi} I_m^\alpha(\rho_t), \quad (82)$$

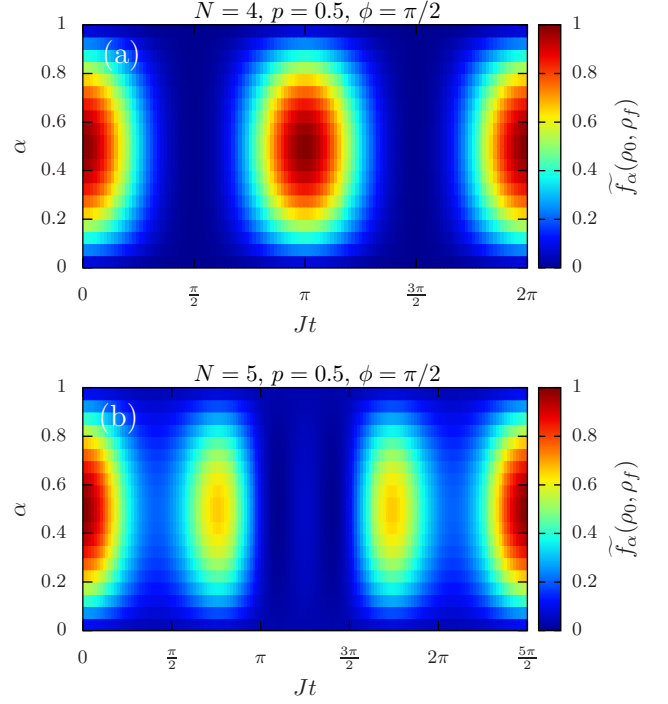


FIG. 7. (Color online) Density plot of normalized relative purity,  $\widetilde{f}_\alpha(\rho_0, \rho_f)$ , for states  $\rho_0$  and  $\rho_f = \mathcal{U}_t^\dagger R_\phi \mathcal{U}_t \rho_0 \mathcal{U}_t R_\phi^\dagger \mathcal{U}_t$ . Here we have  $\mathcal{U}_t = e^{-itH_{zz}}$ , with  $H_{zz} = (J/N) \sum_{j<l} \sigma_j^z \sigma_l^z$  standing as the fully connected Ising Hamiltonian, and also  $R_\phi = e^{-i\phi \hat{S}_x}$ , where  $\hat{S}_x = (1/2) \sum_{i=1}^N \mathbb{I}^{\otimes i-1} \otimes \sigma_i^x \otimes \mathbb{I}^{\otimes N-i}$ . The input state is  $\rho_0 = ((1-p)/d) \mathbb{I} + p(|+\rangle\langle +|)^{\otimes N}$ , with  $d = 2^N$  and  $|+\rangle = (1/\sqrt{2})(|0\rangle + |1\rangle)$ . For simplicity, here we set  $p = 0.5$  and  $\phi = \pi/2$ , and increase the size of the system as (a)  $N = 4$ , and (b)  $N = 5$ .

where

$$I_m^\alpha(\rho_t) = \text{Tr} \left( [(\rho_t)_m^{(\alpha)}]^\dagger (\rho_t)_m^{(1-\alpha)} \right), \quad (83)$$

with

$$(\rho_t)_m^{(\alpha)} := \sum_{\lambda_j - \lambda_\ell = m} \langle j | \rho_t^{(\alpha)} | \ell \rangle \langle j | \ell \rangle. \quad (84)$$

From Sec. III, we recall that  $c_\alpha^{-1} = \text{Tr}(\rho_t^\alpha) = \text{Tr}(\rho_0^\alpha)$ , where we have used that  $\rho_t^\alpha = \mathcal{U}_t \rho_0^\alpha \mathcal{U}_t^\dagger$ . Furthermore, we stress that  $\{|j\rangle\}_{j=1,\dots,2^N}$  describe the *reference basis* generated by the eigenstates of  $\hat{S}_x$ , with their respective set of eigenvalues  $\vec{\lambda} = \{-N/2, -N/2 + 1, \dots, N/2 - 1, N/2\}$  which exhibits degeneracy  $g_{\lambda_j} = N! / [(N/2 + \lambda_j)! (N/2 - \lambda_j)!]$ , and thus  $m = \{-N, -N + 1, \dots, N - 1, N\}$ .

We now apply the above discussion to numerically study the time-evolution of normalized  $\alpha$ -MQI spectrum,  $\{\widetilde{I}_m^\alpha(\rho_t)\}$ , and its the second moment  $\widetilde{F}_I^\alpha(\rho_t, \hat{S}_x)$ . Without loss of generality, here we have adopted the normalization  $\widetilde{G} := (G - \min\{G\}) / (\max\{G\} - \min\{G\})$ .

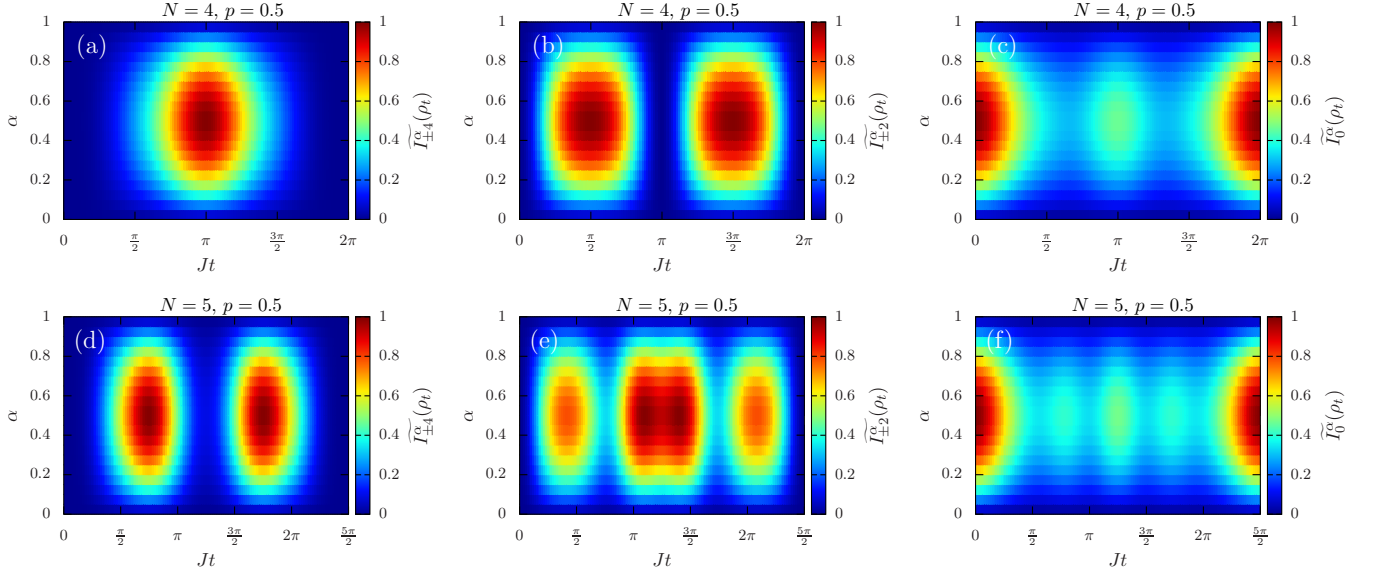


FIG. 8. (Color online) Density plot of normalized  $\alpha$ -MQI,  $\widetilde{I}_m^{\alpha}(\rho_t)$ , for the state  $\rho_t = e^{-itH_{zz}} \rho e^{itH_{zz}}$ , where  $H_{zz} = (J/N) \sum_{j<l} \sigma_j^z \sigma_l^z$  is the fully connected Ising Hamiltonian, and the probe state  $\rho = ((1-p)/d) \mathbb{I} + p(|+\rangle\langle +|)^{\otimes N}$ , with  $d = 2^N$  and  $|+\rangle = (1/\sqrt{2})(|0\rangle + |1\rangle)$ . For simplicity, here we fix the mixing parameter  $p = 0.5$ . The set of non-zero  $\alpha$ -MQI is given by  $\widetilde{I}_{\pm 4}^{\alpha}(\rho_t)$ , for (a)  $N = 4$  and (d)  $N = 5$ ;  $\widetilde{I}_{\pm 2}^{\alpha}(\rho_t)$ , for (b)  $N = 4$  and (e)  $N = 5$ ; and  $\widetilde{I}_0^{\alpha}(\rho_t)$ , for (c)  $N = 4$  and (f)  $N = 5$ .

In Fig. 7 we plot the normalized relative purity,  $\widetilde{f}_{\alpha}(\rho_0, \rho_f) \equiv \widetilde{f}_{\alpha}(\rho_t, \rho_{t,\phi})$  (cf. Eq. (81)), as a function of  $t$  and  $\alpha$ . Just to clarify, here  $\rho_t = e^{-itH_{zz}} \rho_0 e^{itH_{zz}}$ , where  $H_{zz}$  is given in Eq. (79) and  $\rho_0$  is the probe state in Eq. (80), and  $\rho_{t,\phi} = R_{\phi} \rho_t R_{\phi}^{\dagger}$ , with  $R_{\phi} = e^{-i\phi \hat{S}_x}$  and  $\hat{S}_x = (1/2) \sum_{l=1}^N \mathbb{I}^{\otimes l-1} \otimes \sigma_l^x \otimes \mathbb{I}^{\otimes N-l}$ . We fix the mixing parameter  $p = 0.5$ , and the phase  $\phi = \pi/2$ .

In Fig. 8 we plot the time-evolution of the normalized  $\alpha$ -MQI spectrum  $\{\widetilde{I}_m^{\alpha}(\rho_t)\}$  (cf. Eq. (83)) for  $N = 4$  and  $N = 5$ . Given the evolved state  $\rho_t = e^{-itH_{zz}} \rho_0 e^{itH_{zz}}$ , for  $N = 4$  the nonzero  $\alpha$ -MQI are given by (a)  $\widetilde{I}_{\pm 4}^{\alpha}(\rho_t)$ , (b)  $\widetilde{I}_{\pm 2}^{\alpha}(\rho_t)$ , and (c)  $\widetilde{I}_0^{\alpha}(\rho_t)$ . Similarly, for the system size  $N = 5$  the nonzero  $\alpha$ -MQI are given by (d)  $\widetilde{I}_{\pm 4}^{\alpha}(\rho_t)$ , (e)  $\widetilde{I}_{\pm 2}^{\alpha}(\rho_t)$ , and (f)  $\widetilde{I}_0^{\alpha}(\rho_t)$ .

Finally, in Fig. 9 we plot the normalized second moment of  $\alpha$ -MQI spectrum,  $\widetilde{F}_I^{\alpha}(\rho_t, \hat{S}_x)$ , as a function of  $t$  and  $\alpha$ , by varying the size of the system as (a)  $N = 3$ , (b)  $N = 4$ , (c)  $N = 5$ , and (d)  $N = 6$ . As can be seen, time evolution of  $\widetilde{F}_I^{\alpha}(\rho_t, \hat{S}_x)$  oscillates with period  $\pi N/2$ .

## VII. CONCLUSIONS

In conclusion, we have shown that, by considering a quantum system undergoing a unitary phase encoding process, the Rényi relative entropy ( $\alpha$ -RRE) is linked to the well known Wigner-Yanase-Dyson skew information (WYDSI). We further provided a novel framework ad-

ressing the coherence orders of a quantum state with respect to the eigenbasis of an observable  $\hat{A}$ . We introduced the  $\alpha$ -Multiple Quantum Intensity ( $\alpha$ -MQI),  $I_m^{\alpha}(\rho)$ , which is intimately linked to  $\alpha$ -RRE, and thus proved that WYDSI can be also written as the second moment of multiple quantum coherence spectrum ( $\alpha$ -MQC),  $F_I^{\alpha}(\rho, \hat{A})$ .

The second main result concerns the derivation of a family of lower and upper bounds to the second moment of  $\alpha$ -MQI. Interestingly, we have shown that  $F_I^{\alpha}(\rho, \hat{A})$  provides a lower bound on the quantum Fisher information. Noteworthy, bridging  $\alpha$ -MQC and QFI has a number of implications. On one hand, this link unveils the role of the second moment of  $\alpha$ -MQI in quantum phase estimation and metrology. On the other hand, it demonstrates that the second moment of  $\alpha$ -MQI can also witness multiparticle entanglement.

Finally, we illustrate our main results by investigating the single qubit state, Bell-diagonal states, and some paradigmatic multiparticle states. We numerically studied the time evolution of  $\alpha$ -MQC spectrum and the overall signal of relative purity, by simulating the time reversal dynamics of a many-body all-to-all Ising Hamiltonian. Interestingly, dynamical behaviour of  $\alpha$ -MQC unveils information about buildup of many-body correlations, and also signals the recently claimed property of quantum information scrambling [18, 19]. Our results might also find applications in the field of quantum thermodynamics, regarding the family of second laws of thermodynamics parametrized by  $\alpha$ -RRE which was a-



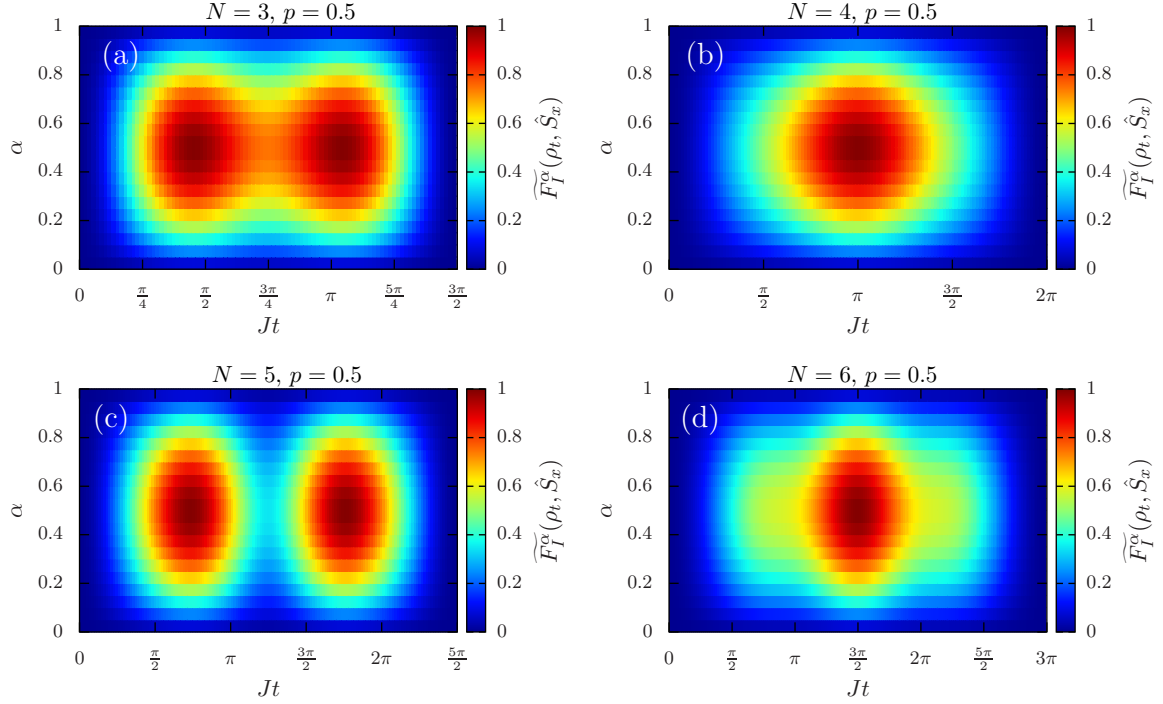


FIG. 9. (Color online) Density plot of normalized second moment of  $\alpha$ -MQI, i.e.,  $\widetilde{F}_I^\alpha(\rho_t, \hat{S}_x)$ , related to the generator  $S_x = (1/2) \sum_{l=1}^N \mathbb{I}^{\otimes l-1} \otimes \sigma_l^x \otimes \mathbb{I}^{\otimes N-l}$  and the evolved state  $\rho_t = e^{-itH_{zz}} \rho e^{itH_{zz}}$ , where  $H_{zz} = (J/N) \sum_{j<l} \sigma_j^z \sigma_l^z$  is the fully connected Ising Hamiltonian. Here we choose the initial state of the system as  $\rho = ((1-p)/d) \mathbb{I} + p(|+\rangle\langle+|)^{\otimes N}$ , with  $d = 2^N$  and  $|+\rangle = (1/\sqrt{2})(|0\rangle + |1\rangle)$ . For simplicity, here we fix  $p = 0.5$  and increase the size of the system as (a)  $N = 3$ , (b)  $N = 4$ , (c)  $N = 5$ , and (d)  $N = 6$ .

ddressed in Refs. [3, 26].

## APPENDIX

### A. PROPERTIES OF $\alpha$ -MQC

In this Appendix we prove Eqs. (8), (9) and (10) of the main text. First, starting from Eq. (7), it is possible to conclude that

$$\begin{aligned}
 (\rho_m^{(\alpha)})^\dagger &= \sum_{\lambda_j - \lambda_\ell = m} \langle j | \rho^{(\alpha)} | \ell \rangle^* | \ell \rangle \langle j | \\
 &= \sum_{\lambda_j - \lambda_\ell = m} \langle \ell | (\rho^{(\alpha)})^\dagger | j \rangle | \ell \rangle \langle j | \\
 &= \sum_{\lambda_\ell - \lambda_j = -m} \langle \ell | \rho^{(\alpha)} | j \rangle | \ell \rangle \langle j | \\
 &= \rho_{-m}^{(\alpha)}. \tag{A1}
 \end{aligned}$$

From second to the third line we have used that  $\rho^{(\alpha)}$  is Hermitian, and from the third to the fourth line we have changed the summation labels.

Now, we show that  $\rho_m^{(\alpha)}$  and  $\rho_n^{(\beta)}$  satisfies an orthogonality constraint with respect to the Hilbert-Schmidt inner product. In order to verify explicitly Eq. (9), one

### ACKNOWLEDGMENTS

We thank T. Roscilde for fruitful discussions. D. P. P. and T. M. acknowledges the financial support from the Brazilian ministries MEC and MCTIC, funding agencies CAPES and CNPq. T. M. acknowledges CNPq for support through Bolsa de produtividade em Pesquisa n.311079/2015-6. This work was supported by the Serapilheira Institute (grant number Serra-1812-27802), CAPES-NUFFIC project number 88887.156521/2017-00. This study was financed by the Coordenação de Aperfeiçoamento de Pessoal de Nível Superior – Brasil (CAPES) – Finance Code 001. This work was also supported by the QuantERA ERA-NET Cofund in Quantum Technologies projects CEBBEC.

may proceed as

$$\begin{aligned}
\langle \rho_m^{(\alpha)} \rho_n^{(\beta)} \rangle_{\text{HS}} &= \\
&= \sum_{\lambda_j - \lambda_\ell = m} \sum_{\lambda_p - \lambda_q = n} \langle j | \rho^{(\alpha)} | \ell \rangle^* \langle p | \rho^{(\beta)} | q \rangle \langle q | \ell \rangle \langle j | p \rangle \\
&= \sum_{\lambda_j - \lambda_\ell = m} \sum_{\lambda_p - \lambda_q = n} \delta_{q,\ell} \delta_{j,p} \langle j | \rho^{(\alpha)} | \ell \rangle^* \langle p | \rho^{(\beta)} | q \rangle \\
&= \sum_{\lambda_j - \lambda_\ell = m} \sum_{\lambda_j - \lambda_\ell = n} \langle j | \rho^{(\alpha)} | \ell \rangle^* \langle j | \rho^{(\beta)} | \ell \rangle . \quad (\text{A2})
\end{aligned}$$

where  $\langle A, B \rangle_{\text{HS}} := \text{Tr}(A^\dagger B)$ , for  $A, B \in \mathcal{B}(\mathcal{H})$ , denotes the Hilbert-Schmidt inner product. Going into details, from the first to the second line we have applied the cyclic permutation under the trace, and from the second to the third line we used  $\langle r | s \rangle = \delta_{r,s}$ . From Eq. (A2), one may conclude that the double summation is nonzero, only for  $m = n$ . Indeed, given two fixed integers  $m$  and  $n$ , such selection rule comes from the fact that both constraints  $\lambda_j - \lambda_\ell = m$  and  $\lambda_j - \lambda_\ell = n$  are simultaneously fulfilled if, and only if,  $m = n$ . Therefore, we readily obtain

$$\begin{aligned}
\langle \rho_m^{(\alpha)} \rho_n^{(\beta)} \rangle_{\text{HS}} &= \delta_{m,n} \sum_{\lambda_j - \lambda_\ell = m} \langle j | \rho^{(\alpha)} | \ell \rangle^* \langle j | \rho^{(\beta)} | \ell \rangle \\
&= \delta_{m,n} \langle \rho_m^{(\alpha)} \rho_m^{(\beta)} \rangle_{\text{HS}} . \quad (\text{A3})
\end{aligned}$$

Finally, we will conclude by proving Eq. (10). Suppose now that the density matrix  $\rho^{(\alpha)}$  undergoes the translationally-covariant evolution  $\mathcal{U}_\phi(\bullet) := e^{-i\phi\hat{A}} \bullet e^{i\phi\hat{A}}$  generated by the observable  $\hat{A}$ . Hence, starting from Eq. (6) in the main text, one gets

$$\mathcal{U}_\phi(\rho^{(\alpha)}) = \sum_m \mathcal{U}_\phi(\rho_m^{(\alpha)}) . \quad (\text{A4})$$

By using Eq. (7) it is possible to write

$$\begin{aligned}
\mathcal{U}_\phi(\rho_m^{(\alpha)}) &= \sum_{\lambda_j - \lambda_\ell = m} \langle j | \rho^{(\alpha)} | \ell \rangle e^{-i\phi\hat{A}} | j \rangle \langle \ell | e^{i\phi\hat{A}} \\
&= e^{-im\phi} \sum_{\lambda_j - \lambda_\ell = m} \langle j | \rho^{(\alpha)} | \ell \rangle | j \rangle \langle \ell | \\
&= e^{-im\phi} \rho_m^{(\alpha)} , \quad (\text{A5})
\end{aligned}$$

where  $m = \lambda_j - \lambda_\ell$ . We stress that from the second to the third line, we used that  $\hat{A}|\ell\rangle = \lambda_\ell|\ell\rangle$  since  $|\ell\rangle$  is an eigenstate of the operator  $\hat{A}$ . Therefore, by substituting Eq. (A5) into (A4) we finally obtain the result

$$\mathcal{U}_\phi(\rho^{(\alpha)}) = \sum_m e^{-im\phi} \rho_m^{(\alpha)} . \quad (\text{A6})$$

## B. LIMITING CASE OF RELATIVE RÉNYI ENTROPY FOR $\alpha \rightarrow 1$

In this Appendix we investigate the behaviour of Eq. (19) when taking the limit  $\alpha \rightarrow 1$ . Given the states  $\rho$

and  $\rho_\phi = e^{i\phi\hat{A}} \rho e^{-i\phi\hat{A}}$ , the Taylor expansion of  $\alpha$ -relative Rényi entropy up to second order in  $\phi$ , around  $\phi = 0$ , becomes

$$D_\alpha(\rho || \rho_\phi) \approx -\frac{\phi^2}{\alpha - 1} \mathcal{I}_\alpha(\rho, \hat{A}) + O(\phi^3) , \quad (\text{B1})$$

where  $\mathcal{I}_\alpha(\rho, \hat{A})$  stands for the Wigner-Yanase-Dyson skew information (WYDSI) and, according Eq. (20), is also written as

$$\mathcal{I}_\alpha(\rho, \hat{A}) = \text{Tr}(\rho \hat{A}^2) - \text{Tr}(\rho^\alpha \hat{A} \rho^{1-\alpha} \hat{A}) . \quad (\text{B2})$$

In particular, note that WYDSI vanishes for  $\alpha = 1$ . In this case, for  $\alpha \rightarrow 1$  the right-hand side of Eq. (B1) will exhibit an indeterminacy form as  $\frac{0}{0}$ . Notably, one may formally circumvent this issue by applying l'Hôpital rule, which implies the prior differentiation of both numerator and denominator with respect to  $\alpha$ , and finally take the limit  $\alpha \rightarrow 1$ . Therefore, one gets

$$\lim_{\alpha \rightarrow 1} D_\alpha(\rho || \rho_\phi) \approx -\phi^2 \lim_{\alpha \rightarrow 1} \frac{\frac{d}{d\alpha} \mathcal{I}_\alpha(\rho, \hat{A})}{\frac{d}{d\alpha}(\alpha - 1)} + O(\phi^3) . \quad (\text{B3})$$

The denominator in the right-hand side of Eq. (B3) is well behaved and approaches 1 as  $\alpha \rightarrow 1$ . Moving to the numerator, to determine explicitly the derivative of WYDSI with respect to  $\alpha$ , we shall begin by simplifying the quantity  $\mathcal{I}_\alpha(\rho, \hat{A})$ . Let  $\rho = \sum_\ell p_\ell |\psi_\ell\rangle \langle \psi_\ell|$  be the spectral decomposition of the density matrix into the basis  $\{|\psi_\ell\rangle\}_{\ell=1,\dots,d}$ , with  $0 \leq p_\ell \leq 1$ ,  $\text{Tr}(\rho) = \sum_\ell p_\ell = 1$ , and  $\langle \psi_j | \psi_\ell \rangle = \delta_{j,\ell}$  for all  $j, \ell$ . In this case, it is straightforward to verify that

$$\text{Tr}(\rho \hat{A}^2) = \sum_{j,\ell} p_j |\langle \psi_j | \hat{A} | \psi_\ell \rangle|^2 , \quad (\text{B4})$$

and

$$\text{Tr}(\rho^\alpha \hat{A} \rho^{1-\alpha} \hat{A}) = \sum_{j,\ell} p_j^\alpha p_\ell^{1-\alpha} |\langle \psi_j | \hat{A} | \psi_\ell \rangle|^2 . \quad (\text{B5})$$

By substituting Eqs. (B4) and (B5) into Eq. (B2), and also using that  $p_j - p_j^\alpha p_\ell^{1-\alpha} = p_j^\alpha (p_j^{1-\alpha} - p_\ell^{1-\alpha})$ , one obtains

$$\mathcal{I}_\alpha(\rho, \hat{A}) = \sum_{j,\ell} p_j^\alpha (p_j^{1-\alpha} - p_\ell^{1-\alpha}) |\langle \psi_j | \hat{A} | \psi_\ell \rangle|^2 . \quad (\text{B6})$$

To differentiate WYDSI with respect to  $\alpha$ , we will take advantage from the algebraic identity  $d p_j^\alpha / d\alpha = p_j^\alpha \ln p_j$ . Hence, by combining this result with the derivative of Eq. (B6), it is straightforward to conclude that

$$\begin{aligned}
\lim_{\alpha \rightarrow 1} \frac{d}{d\alpha} \mathcal{I}_\alpha(\rho, \hat{A}) &= \sum_{j,\ell} p_j (\ln p_\ell - \ln p_j) |\langle \psi_j | \hat{A} | \psi_\ell \rangle|^2 \\
&= \text{Tr}(\hat{A} \rho \hat{A} \ln \rho) - \text{Tr}(\hat{A}^2 \rho \ln \rho) . \quad (\text{B7})
\end{aligned}$$

Finally, from Eq. (B7) one may readily simplify Eq. (B3) and obtain the limiting case  $\alpha \rightarrow 1$  of Taylor expansion of relative Rényi entropy as follows

$$\lim_{\alpha \rightarrow 1} D_\alpha(\rho || \rho_\phi) \approx \phi^2 \left( \text{Tr}(\hat{A}^2 \rho \ln \rho) - \text{Tr}(\hat{A} \rho \hat{A} \ln \rho) \right) + O(\phi^3) . \quad (\text{B8})$$

### C. LOWER BOUND FOR WYDSI

In this Appendix we will investigate some bounds on Wigner-Yanase-Dyson skew information (WYDSI). To begin, we notice that, from Eq. (B6), WYDSI also read as

$$\mathcal{I}_\alpha(\rho, \hat{A}) = \sum_{j < \ell} (p_j^\alpha - p_\ell^\alpha) (p_j^{1-\alpha} - p_\ell^{1-\alpha}) |\langle \psi_j | \hat{A} | \psi_\ell \rangle|^2, \quad (\text{C1})$$

which comes from the fact that, since  $\hat{A}$  is a Hermitian operator, thus the amplitude  $|\langle j | \hat{A} | \ell \rangle|^2$  remains invariant under changing labels  $j \rightarrow \ell$ . In particular, for  $\alpha = 1/2$  Eq. (C1) becomes

$$\mathcal{I}_{1/2}(\rho, \hat{A}) = \sum_{j < \ell} (\sqrt{p_j} - \sqrt{p_\ell})^2 |\langle \psi_j | \hat{A} | \psi_\ell \rangle|^2. \quad (\text{C2})$$

Now, we address the quantifier  $\mathcal{I}^L(\rho, \hat{A})$ , which can be written as

$$\mathcal{I}^L(\rho, \hat{A}) = \frac{1}{2} \left( \text{Tr}(\rho^2 \hat{A}^2) - \text{Tr}(\rho \hat{A} \rho \hat{A}) \right). \quad (\text{C3})$$

In turn, notice that

$$\text{Tr}(\rho^2 \hat{A}^2) = \sum_{j, \ell} p_j^2 |\langle \psi_j | \hat{A} | \psi_\ell \rangle|^2, \quad (\text{C4})$$

and

$$\text{Tr}(\rho \hat{A} \rho \hat{A}) = \sum_{j, \ell} p_j p_\ell |\langle \psi_j | \hat{A} | \psi_\ell \rangle|^2. \quad (\text{C5})$$

Thus, by substituting Eqs. (C4) and (C5) into Eq. (C3), we obtain

$$\mathcal{I}^L(\rho, \hat{A}) = \frac{1}{2} \sum_{j, \ell} p_j (p_j - p_\ell) |\langle \psi_j | \hat{A} | \psi_\ell \rangle|^2. \quad (\text{C6})$$

Once more, as the amplitude  $|\langle j | \hat{A} | \ell \rangle|^2$  is invariant under changing labels  $j \rightarrow \ell$ , one gets

$$\mathcal{I}^L(\rho, \hat{A}) = \frac{1}{2} \sum_{j < \ell} (p_j - p_\ell)^2 |\langle \psi_j | \hat{A} | \psi_\ell \rangle|^2. \quad (\text{C7})$$

Some remarks are now in order. Yanagi [85] (see Lemma 3.3) has proved that for any  $x > 0$  and  $0 \leq \alpha \leq 1$ , the following inequality holds

$$(1 - 2\alpha)^2 (x - 1)^2 - (x^\alpha - x^{1-\alpha})^2 \geq 0. \quad (\text{C8})$$

Interestingly, we stress that Eq. (C8) can be also written as

$$4\alpha(1-\alpha)(1-x)^2 \leq (1-x^\alpha)(1-x^{1-\alpha})\kappa_\alpha(x), \quad (\text{C9})$$

where we define

$$\kappa_\alpha(x) := 1 + x + x^\alpha + x^{1-\alpha} \quad (\text{C10})$$

From now on, we will focus mainly on Eq. (C10) in the search of a new class of bounds to WYDSI. According to Heinz inequality [97, 98], for  $a > 0$ ,  $b > 0$  and  $0 < \alpha < 1$ , the following inequality holds

$$a^\alpha b^{1-\alpha} + a^{1-\alpha} b^\alpha \leq a + b. \quad (\text{C11})$$

In special, by choosing  $x = a/b$ , with  $x > 0$ , Eq. (C11) becomes

$$x^\alpha + x^{1-\alpha} \leq 1 + x. \quad (\text{C12})$$

Hence, Eq. (C12) allows us to conclude the bound

$$\kappa_\alpha(x) \leq 2(1+x). \quad (\text{C13})$$

By substituting Eq. (C13) into Eq. (C9), it yields the new bound

$$2\alpha(1-\alpha)(1-x)^2 \leq (1+x)(1-x^\alpha)(1-x^{1-\alpha}). \quad (\text{C14})$$

We would like to stress that bound in Eq. (C14) applies to any  $x > 0$  and  $0 \leq \alpha \leq 1$ .

Starting from Eq. (C14), let us choose  $x = p_j/p_\ell$ , with  $x > 0$ , and  $0 < p_j \leq 1$  and  $0 < p_\ell \leq 1$ . In this case, it is straightforward to write down the inequality

$$2\alpha(1-\alpha)(p_j - p_\ell)^2 \leq (p_j + p_\ell)(p_j^\alpha - p_\ell^\alpha)(p_j^{1-\alpha} - p_\ell^{1-\alpha}). \quad (\text{C15})$$

Hence, by substituting Eq. (C15) into Eq. (C7), one may conclude that

$$\begin{aligned} 2\alpha(1-\alpha)\mathcal{I}^L(\rho, \hat{A}) &= \sum_{j < \ell} \alpha(1-\alpha)(p_j - p_\ell)^2 |\langle \psi_j | \hat{A} | \psi_\ell \rangle|^2 \\ &\leq \frac{1}{2} \sum_{j < \ell} (p_j + p_\ell)(p_j^\alpha - p_\ell^\alpha)(p_j^{1-\alpha} - p_\ell^{1-\alpha}) |\langle \psi_j | \hat{A} | \psi_\ell \rangle|^2. \end{aligned} \quad (\text{C16})$$

Now we approach a crucial point in our derivation. Going into details, RHS in Eq. (C16) will exactly recover Wigner-Yanase-Dyson skew information in Eq. (C1) if we turn to the fact that  $p_j + p_\ell \leq 2$  for all  $0 < p_j \leq 1$  and  $0 < p_\ell \leq 1$ . Therefore, applying such a result into Eq. (C16), we obtain

$$\begin{aligned} 2\alpha(1-\alpha)\mathcal{I}^L(\rho, \hat{A}) &\leq \\ &\sum_{j < \ell} (p_j^\alpha - p_\ell^\alpha)(p_j^{1-\alpha} - p_\ell^{1-\alpha}) |\langle \psi_j | \hat{A} | \psi_\ell \rangle|^2. \end{aligned} \quad (\text{C17})$$

Finally, it is straightforward to obtain the lower bound

$$\mathcal{I}_\alpha(\rho, \hat{A}) \geq 2\alpha(1-\alpha)\mathcal{I}^L(\rho, \hat{A}). \quad (\text{C18})$$

- 
- [1] L. Jaeger, *The Second Quantum Revolution* (Springer, New York, 2018).
- [2] J. Åberg, “Catalytic coherence,” *Phys. Rev. Lett.* **113**, 150402 (2014).
- [3] P. Ćwikliński, M. Studziński, M. Horodecki, and J. Oppenheim, “Limitations on the Evolution of Quantum Coherences: Towards Fully Quantum Second Laws of Thermodynamics,” *Phys. Rev. Lett.* **115**, 210403 (2015).
- [4] G. Karpat, B. Çakmak, and F. F. Fanchini, “Quantum coherence and uncertainty in the anisotropic XY chain,” *Phys. Rev. B* **90**, 104431 (2014).
- [5] A. L. Malvezzi, G. Karpat, B. Çakmak, F. F. Fanchini, T. Debarba, and R. O. Vianna, “Quantum correlations and coherence in spin-1 Heisenberg chains,” *Phys. Rev. B* **93**, 184428 (2016).
- [6] S. F. Huelga and M. B. Plenio, “Quantum biology: A vibrant environment,” *Nat. Phys.* **10**, 621 (2014).
- [7] J. J. J. Roden, D. I. G. Bennett, and K. B. Whaley, “Long-range energy transport in photosystem II,” *J. Chem. Phys.* **144**, 245101 (2016).
- [8] A. Streltsov, G. Adesso, and M. B. Plenio, “Colloquium: Quantum coherence as a resource,” *Rev. Mod. Phys.* **89**, 041003 (2017).
- [9] M. Munowitz, *Coherence and NMR* (John Wiley & Sons, Cambridge, 1988).
- [10] J. Keeler, *Understanding NMR Spectroscopy*, 2nd ed. (John Wiley & Sons, Cambridge, 2010).
- [11] J. Baum, M. Munowitz, A. N. Garroway, and A. Pines, “Multiple-quantum dynamics in solid state NMR,” *J. Chem. Phys.* **83**, 2015 (1985).
- [12] M. Munowitz and A. Pines, “Multiple-Quantum Nuclear Magnetic Resonance Spectroscopy,” *Science* **233**, 525 (1986).
- [13] J. Baum and A. Pines, “NMR studies of clustering in solids,” *J. Am. Chem. Soc.* **108**, 7447 (1986).
- [14] A. K. Khitrin, “Growth of NMR multiple-quantum coherences in quasi-one-dimensional systems,” *Chem. Phys. Lett.* **274**, 217 (1997).
- [15] G. A. Álvarez and D. Suter, “Localization effects induced by decoherence in superpositions of many-spin quantum states,” *Phys. Rev. A* **84**, 012320 (2011).
- [16] G. B. Furman, V. M. Meerovich, and V. L. Sokolovsky, “Multiple quantum NMR and entanglement dynamics in dipolar coupling spin systems,” *Phys. Rev. A* **78**, 042301 (2008).
- [17] D. P. Pires, I. A. Silva, E. R. deAzevedo, D. O. Soares-Pinto, and J. G. Filgueiras, “Coherence orders, decoherence, and quantum metrology,” *Phys. Rev. A* **98**, 032101 (2018).
- [18] M. Gärttner, P. Hauke, and A. M. Rey, “Relating Out-of-Time-Order Correlations to Entanglement via Multiple-Quantum Coherences,” *Phys. Rev. Lett.* **120**, 040402 (2018).
- [19] M. Gärttner, J. Bohnet, A. Safavi-Naini, M. L. Wall, J. J. Bollinger, and A. M. Rey, “Measuring out-of-time-order correlations and multiple quantum spectra in a trapped-ion quantum magnet,” *Nature Phys.* **13**, 781 (2017).
- [20] K. X. Wei, C. Ramanathan, and P. Cappellaro, “Exploring Localization in Nuclear Spin Chains,” *Phys. Rev. Lett.* **120**, 070501 (2018).
- [21] C. M. Sánchez, A. K. Chattah, K. X. Wei, L. Buljubasich, P. Cappellaro, and H. M. Pastawski, “Perturbation Independent Decay of the Loschmidt Echo in a Many-Body System,” *Phys. Rev. Lett.* **124**, 030601 (2020).
- [22] M. K. Joshi, A. Elben, B. Vermersch, T. Brydges, C. Maier, P. Zoller, R. Blatt, and C. F. Roos, “Quantum Information Scrambling in a Trapped-ion Quantum Simulator with Tunable Range Interactions,” *Phys. Rev. Lett.* **124**, 240505 (2020).
- [23] K. X. Wei, P. Peng, O. Shtanko, I. Marvian, S. Lloyd, C. Ramanathan, and P. Cappellaro, “Emergent Prethermalization Signatures in Out-of-Time Ordered Correlations,” *Phys. Rev. Lett.* **123**, 090605 (2019).
- [24] J. Li, R. Fan, H. Wang, B. Ye, B. Zeng, H. Zhai, X. Peng, and J. Du, “Measuring Out-of-Time-Order Correlators on a Nuclear Magnetic Resonance Quantum Simulator,” *Phys. Rev. X* **7**, 031011 (2017).
- [25] K. A. Landsman, C. Figgatt, T. Schuster, N. M. Linke, B. Yoshida, N. Y. Yao, and C. Monroe, “Verified quantum information scrambling,” *Nature* **567**, 61 (2019).
- [26] F. Brandão, M. Horodecki, N. Ng, J. Oppenheim, and S. Wehner, “The second laws of quantum thermodynamics,” *Proc. Natl. Acad. Sci.* **112**, 3275 (2015).
- [27] B.-B. Wei and M. B. Plenio, “Relations between dissipated work in non-equilibrium process and the family of Rényi divergences,” *New J. Phys.* **19**, 023002 (2017).
- [28] G. Guarnieri, N. H. Y. Ng, K. Modi, J. Eisert, M. Paternostro, and J. Goold, “Quantum work statistics and resource theories: Bridging the gap through Rényi divergences,” *Phys. Rev. E* **99**, 050101 (2019).
- [29] F. Leditzky, M. M. Wilde, and N. Datta, “Strong converse theorems using Rényi entropies,” *J. Math. Phys.* **57**, 082202 (2016).
- [30] E. Chitambar and G. Gour, “Critical Examination of Incoherent Operations and a Physically Consistent Resource Theory of Quantum Coherence,” *Phys. Rev. Lett.* **117**, 030401 (2016).
- [31] E. Chitambar and G. Gour, “Comparison of incoherent operations and measures of coherence,” *Phys. Rev. A* **94**, 052336 (2016).
- [32] A. E. Rastegin, “Quantum-coherence quantifiers based on the Tsallis relative  $\alpha$  entropies,” *Phys. Rev. A* **93**, 032136 (2016).
- [33] A. Streltsov, H. Kampermann, S. Wölk, M. Gessner, and D. Bruß, “Maximal coherence and the resource theory of purity,” *New J. Phys.* **20**, 053058 (2018).
- [34] K. P. Seshadreesan, L. Lami, and M. M. Wilde, “Rényi relative entropies of quantum Gaussian states,” *J. Math. Phys.* **59**, 072204 (2018).
- [35] P. Horodecki and A. Ekert, “Method for Direct Detection of Quantum Entanglement,” *Phys. Rev. Lett.* **89**, 127902 (2002).
- [36] J. Cardy, “Measuring Entanglement Using Quantum Quenches,” *Phys. Rev. Lett.* **106**, 150404 (2011).
- [37] D. A. Abanin and E. Demler, “Measuring Entanglement Entropy of a Generic Many-Body System with a Quantum Switch,” *Phys. Rev. Lett.* **109**, 020504 (2012).
- [38] A. Elben, R. Kueng, H.-Y. Huang, R. van Bijnen, C. Kokail, M. Dalmonte, P. Calabrese, B. Kraus, J. Preskill, P. Zoller, and B. Vermersch, “Mixed-state entanglement from local randomized measurements,”

- arXiv:2007.06305.
- [39] A. Elben, B. Vermersch, M. Dalmonte, J. I. Cirac, and P. Zoller, “Rényi Entropies from Random Quenches in Atomic Hubbard and Spin Models,” *Phys. Rev. Lett.* **120**, 050406 (2018).
- [40] R. Islam, R. Ma, P. M. Preiss, M. E. Tai, A. Lukin, M. Rispoli, and M. Greiner, “Measuring entanglement entropy in a quantum many-body system,” *Nature (London)* **528**, 77 (2015).
- [41] N. M. Linke, S. Johri, C. Figgatt, K. A. Landsman, A. Y. Matsuura, and C. Monroe, “Measuring the Rényi entropy of a two-site Fermi-Hubbard model on a trapped ion quantum computer,” *Phys. Rev. A* **98**, 052334 (2018).
- [42] T. Brydges, A. Elben, P. Jurcevic, B. Vermersch, C. Maier, B. P. Lanyon, P. Zoller, R. Blatt, and C. F. Roos, “Probing Rényi entanglement entropy via randomized measurements,” *Science* **364**, 260 (2019).
- [43] A. J. Daley, H. Pichler, J. Schachenmayer, and P. Zoller, “Measuring Entanglement Growth in Quench Dynamics of Bosons in an Optical Lattice,” *Phys. Rev. Lett.* **109**, 020505 (2012).
- [44] I. Frérôt and T. Roscilde, “Quantum variance: A measure of quantum coherence and quantum correlations for many-body systems,” *Phys. Rev. B* **94**, 075121 (2016).
- [45] J. S. Sidhu and P. Kok, “Geometric perspective on quantum parameter estimation,” *AVS Quantum Sci.* **2**, 014701 (2020).
- [46] L. Pezzé and A. Smerzi, “Entanglement, Nonlinear Dynamics, and the Heisenberg Limit,” *Phys. Rev. Lett.* **102**, 100401 (2009).
- [47] L. Pezzé and A. Smerzi, “Quantum theory of phase estimation,” in *Atom Interferometry, Proceedings of the International School of Physics “Enrico Fermi”*, Vol. 188, edited by G. M. Tino and M. A. Kasevich (IOS Press, Amsterdam, 2014) pp. 691–741.
- [48] D. Petz, “Quasi-entropies for States of a von Neumann Algebra,” *Publ. Res. Inst. Math. Sci.* **21**, 787 (1985).
- [49] D. Petz, “Quasi-entropies for finite quantum systems,” *Rep. Math. Phys.* **23**, 57 (1986).
- [50] M. Mosonyi and F. Hiai, “On the Quantum Rényi Relative Entropies and Related Capacity Formulas,” *IEEE Trans. Inf. Theory* **57**, 2474 (2011).
- [51] M. Müller-Lennert, F. Dupuis, O. Szehr, S. Fehr, and M. Tomamichel, “On quantum Rényi entropies: A new generalization and some properties,” *J. Math. Phys.* **54**, 122203 (2013).
- [52] F. Leditzky, C. Rouzé, and N. Datta, “Data processing for the sandwiched Rényi divergence: a condition for equality,” *Lett. Math. Phys.* **107**, 61 (2017).
- [53] M. Mosonyi and T. Ogawa, “Quantum Hypothesis Testing and the Operational Interpretation of the Quantum Rényi Relative Entropies,” *Commun. Math. Phys.* **334**, 1617 (2015).
- [54] I. Csiszár, “Information-type measures of difference of probability distributions and indirect observations,” *Studia Sci. Math. Hungar.* **2**, 299 (1967).
- [55] F. Hiai, M. Ohya, and M. Tsukada, “Sufficiency, KMS condition and relative entropy in von Neumann algebras,” *Pacific J. Math.* **96**, 99 (1981).
- [56] G. L. Gilardoni, “On Pinsker’s and Vajda’s Type Inequalities for Csiszár’s  $f$ -Divergences,” *IEEE Trans. Inf. Theory* **56**, 5377 (2010).
- [57] A. E. Rastegin, “Bounds of the Pinsker and Fannes Types on the Tsallis Relative Entropy,” *Math. Phys. Anal. Geom.* **16**, 213 (2013).
- [58] M. M. Wilde, A. Winter, and D. Yang, “Strong Converse for the Classical Capacity of Entanglement-Breaking and Hadamard Channels via a Sandwiched Rényi Relative Entropy,” *Commun. Math. Phys.* **331**, 593 (2014).
- [59] K. M. R. Audenaert, “Comparisons between quantum state distinguishability measures,” *Quantum Inf. Comput.* **14**, 31 (2014).
- [60] K. M. R. Audenaert, J. Calsamiglia, R. Muñoz Tapia, E. Bagan, Ll. Masanes, A. Acín, and F. Verstraete, “Discriminating States: The Quantum Chernoff Bound,” *Phys. Rev. Lett.* **98**, 160501 (2007).
- [61] R. T. Powers and E. Størmer, “Free states of the canonical anticommutation relations,” *Commun. Math. Phys.* **16**, 1 (1970).
- [62] V. Jakšić, Y. Ogata, C.-A. Pillet, and R. Seiringer, “Quantum Hypothesis Testing and Non-Equilibrium Statistical Mechanics,” *Rev. Math. Phys.* **24**, 1230002 (2012).
- [63] H. Umegaki, “Conditional expectation in an operator algebra. IV. Entropy and information,” *Kodai Math. Sem. Rep.* **14**, 59 (1962).
- [64] T van Erven and P. Harremoës, “Rényi Divergence and Kullback-Leibler Divergence,” *IEEE Trans. Inf. Theory* **60**, 3797–3820 (2014).
- [65] N. Datta, “Min- and Max-Relative Entropies and a New Entanglement Monotone,” *IEEE Trans. Inf. Theory* **55**, 2816 (2009).
- [66] I. Marvian and R. W. Spekkens, “How to quantify coherence: Distinguishing speakable and unspeakable notions,” *Phys. Rev. A* **94**, 052324 (2016).
- [67] Rajendra Bathia, *Matrix Analysis* (Springer-Verlag, New York, 1997).
- [68] D. P. Pires, L. C. Céleri, and D. O. Soares-Pinto, “Geometric lower bound for a quantum coherence measure,” *Phys. Rev. A* **91**, 042330 (2015).
- [69] V. Giovannetti, S. Lloyd, and L. Maccone, “Quantum Metrology,” *Phys. Rev. Lett.* **96**, 010401 (2006).
- [70] L. Pezzè, A. Smerzi, M. K. Oberthaler, R. Schmied, and P. Treutlein, “Quantum metrology with nonclassical states of atomic ensembles,” *Rev. Mod. Phys.* **90**, 035005 (2018).
- [71] G. Tóth and I. Apellaniz, “Quantum metrology from a quantum information science perspective,” *J. Phys. A: Math. Theor.* **47**, 424006 (2014).
- [72] R. Jozsa, “Fidelity for Mixed Quantum States,” *J. Mod. Opt.* **41**, 2315 (1994).
- [73] E. P. Wigner and Mutsuo M. Yanase, “Information contents of distributions,” *Proc. Natl. Acad. Sci.* **49**, 910 (1963).
- [74] E. H. Lieb, “Convex trace functions and the Wigner-Yanase-Dyson conjecture,” *Adv. Math.* **11**, 267 (1973).
- [75] E. H. Lieb and M. B. Ruskai, “A Fundamental Property of Quantum-Mechanical Entropy,” *Phys. Rev. Lett.* **30**, 434 (1973).
- [76] R. Takagi, “Skew informations from an operational view via resource theory of asymmetry,” *Sci. Rep.* **9**, 14562 (2019).
- [77] I. Marvian and R. W. Spekkens, “Extending Noether’s theorem by quantifying the asymmetry of quantum states,” *Nature Commun.* **5**, 3821 (2014).
- [78] H. J. D. Miller, M. Scandi, J. Anders, and M. Perarnau-Llobet, “Work Fluctuations in Slow Processes: Quantum



- Signatures and Optimal Control,” *Phys. Rev. Lett.* **123**, 230603 (2019).
- [79] M. Scandi, H. J. D. Miller, J. Anders, and M. Perarnau-Llobet, “Quantum work statistics close to equilibrium,” *Phys. Rev. Research* **2**, 023377 (2020).
- [80] I. M. Mashahd, *Symmetry, asymmetry and quantum information*, Ph.D. thesis, University of Waterloo, 2012.
- [81] K. Macieszczak, E. Levi, T. Macrì, I. Lesanovsky, and J. P. Garrahan, “Coherence, entanglement, and quantumness in closed and open systems with conserved charge, with an application to many-body localization,” *Phys. Rev. A* **99**, 052354 (2019).
- [82] D. Girolami, “Observable Measure of Quantum Coherence in Finite Dimensional Systems,” *Phys. Rev. Lett.* **113**, 170401 (2014).
- [83] C. Zhang, B. Yadin, Z.-B. Hou, H. Cao, B.-H. Liu, Y.-F. Huang, R. Maity, V. Vedral, C.-F. Li, G.-C. Guo, and D. Girolami, “Detecting metrologically useful asymmetry and entanglement by a few local measurements,” *Phys. Rev. A* **96**, 042327 (2017).
- [84] D. Girolami and B. Yadin, “Witnessing Multipartite Entanglement by Detecting Asymmetry,” *Entropy* **19**(3), 124 (2017).
- [85] K. Yanagi, “Wigner-Yanase-Dyson skew information and uncertainty relation,” *J. Phys.: Conf. Ser.* **201**, 012015 (2010).
- [86] S. L. Braunstein and C. M. Caves, “Statistical distance and the geometry of quantum states,” *Phys. Rev. Lett.* **72**, 3439 (1994).
- [87] I. Bengtsson and K. Życzkowski, *Geometry of Quantum States: An Introduction to Quantum Entanglement* (Cambridge University Press, England, 2006).
- [88] S. Luo, “Wigner-Yanase skew information vs. quantum Fisher information,” *Proc. Amer. Math. Soc.* **132**, 885 (2004).
- [89] P. Gibilisco, D. Imparato, and T. Isola, “Inequalities for quantum Fisher information,” *Proc. Amer. Math. Soc.* **137**, 317 (2009).
- [90] R. Horodecki and M. Horodecki, “Information-theoretic aspects of inseparability of mixed states,” *Phys. Rev. A* **54**, 1838 (1996).
- [91] R. Horodecki, P. Horodecki, M. Horodecki, and K. Horodecki, “Quantum entanglement,” *Rev. Mod. Phys.* **81**, 865 (2009).
- [92] W. Dür, G. Vidal, and J. I. Cirac, “Three qubits can be entangled in two inequivalent ways,” *Phys. Rev. A* **62**, 062314 (2000).
- [93] T. Macrì, A. Smerzi, and L. Pezzè, “Loschmidt echo for quantum metrology,” *Phys. Rev. A* **94**, 010102 (2016).
- [94] V. Borish, O. Marković, J. A. Hines, S. V. Rajagopal, and M. Schleier-Smith, “Transverse-Field Ising Dynamics in a Rydberg-Dressed Atomic Gas,” *Phys. Rev. Lett.* **124**, 063601 (2020).
- [95] W.-K. Rhim, A. Pines, and J. S. Waugh, “Time-Reversal Experiments in Dipolar-Coupled Spin Systems,” *Phys. Rev. B* **3**, 684 (1971).
- [96] P. R. Zangara, D. Bendersky, P. R. Levstein, and H. M. Pastawski, “Loschmidt echo in many-spin systems: contrasting time scales of local and global measurements,” *Phil. Trans. R. Soc. A* **374**, 20150163 (2016).
- [97] R. Bhatia, “Interpolating the arithmetic-geometric mean inequality and its operator version,” *Lin. Alg. Appl.* **413**, 355 (2006).
- [98] K. Audenaert, “A singular value inequality for Heinz means,” *Lin. Alg. Appl.* **422**, 279 (2007)